GEOCHEMICAL INVESTIGATIONS OF RESPIRABLE PARTICULATE MATTER

Joseph Bernard Jurinski

Dissertation submitted to the Faculty of the
Virginia Polytechnic Institute and State University
in partial fulfillment of the requirements for the degree of

Doctor of Philosophy
in
Geological Sciences

J. Donald Rimstidt, Chair
James R. Craig
Harry Mahar
Paul H. Ribbe
Harold E. Seifried

June 10, 1998

Blacksburg, Virginia

Keywords: Biodurability, Bioavailability, Respirable, Talc, Coal Fly Ash, Arsenic, Chromium, Health Effects, Mineral Dusts

GEOCHEMICAL INVESTIGATIONS OF RESPIRABLE PARTICULATE MATTER

Joseph Bernard Jurinski

(Abstract)

Over the course of our lives we are exposed to airborne particulate matter in the workplace, home, and environment that results in the deposition of millions of particles in the lung. These exposures may result in disease if they are significant enough. The potential for harmful exposure depends in part on the dust's biodurability and the bioavailability of harmful constituents derived from the particles. A mixed flow reactor was used to evaluate two applications of geochemical methods to characterize the behavior of inhaled particles in the body. Dissolution rates of a well-characterized sample of powdered talc were measured in solvents that mimic fluids found in the human lung. These studies showed that variation of solvent chemistry, including the addition of organic chelators and proteins at intercellular fluid concentrations, does not markedly affect the measured dissolution rate of talc at 37°C and the data further indicate that the dissolution mechanism for talc in aqueous solutions is independent of pH over a range of pH from 2 to 8. The dissolution rate, determined by measuring the silicon release rate per unit surface area of talc is 1.4 (± 1.0) x 10^{-11} mol Si/(m^2 -sec). A geometric shrinking particle model using this dissolution rate predicts an estimated lifetime (upper limit) of approximately 8 years for a 1 micron talc particle under pulmonary conditions. Talc dissolves considerably faster than quartz, but slower than chrysotile and olivine in the body. These data can be used to place constraints on the role of particle dissolution in the disease models associated with airborne respirable particulate matter.

Secondly, the bioavailability of As and Cr was determined from a sample of coal fly ash from an eastern U.S. power plant. The time-release profiles of As and Cr were determined for these materials in physiologically-based solvents and incorporated into a toxicokinetic model to predict the exposure

potential to As and Cr from occupational exposures to the coal fly ash. Predicted occupational exposure contributions from the ash relative to total environmental exposures were insignificant. The exposure predicted from the geochemical approach was compared with results observed in a cohort occupationally exposed to coal fly ash and found to be within one order of magnitude of the response of the occupational cohort. These results support the application of geochemical techniques to evaluate exposures to complex respirable materials.

ACKNOWLEDGMENTS

Where to begin? This project would not have been possible where it not for the patience of Don Rimstidt, who put up with the slow progress over the years. I owe a debt of gratitude for his insightful input into this project and his willingness to oversee a project bridging two disciplines. Thoughtful review and guidance were also provided by my committee members, and I wish to thank Drs. Jim Craig, Harry Mahar, Paul Ribbe, and Harry Seifried for their constructive and timely input. Laboratory support was graciously provided by Dr. Hugh Granger of HP Environmental, Inc. and Bryan Mason of the Industrial Hygiene Laboratory of American Medical Laboratories, Inc. Both welcomed me in their laboratories and provided valuable support on this project. Mark Watson provided access when needed to the transmission electron microscope at Mantech International, Inc's Rockville, Maryland laboratory.

On a personal note, I wish to thank Llyn Sharp and Dan Sable for always leaving the door open and giving me a place to stay when I needed to come down to Blacksburg. I also wish to thank my parents, Neil and Sheila, for their support through this effort. Finally, I wish to thank my wife, Wendy, for her persistent nudging and patience, even when I converted the laundry room to a laboratory and the experiments escaped their containers and leaked across the basement floor!

TABLE OF CONTENTS

TITLE PAGE ..... **i**
ABSTRACT ..... **ii**
ACKNOWLEDGMENTS ..... **iv**
TABLE OF CONTENTS ..... **v**
CHAPTER 1: INTRODUCTION **1**
References 6
CHAPTER 2: BIODURABILITY OF TALC **8**
Abstract 8
Introduction 9
Previous Studies 11
Methods 12
Talc Sample 12
Surface Area Analysis 12
Solvent Preparation 13
Mixed Flow Reactor Method 14
Silica Analysis 14
Analytical Results 15
Discussion 18
Conclusions 24
Acknowledgments 24
References 25
CHAPTER 3: BIOAVAILABILITY OF ARSENIC AND CHROMIUM FROM COAL FLY ASH **27**
Abstract 27
Introduction 28
Methods 30
Characterization of the ash sample 30
Solution preparation, reaction and analysis 33
Analytical Results 36
Discussion 42
Industrial Hygiene 42
Conceptual Model 46
Experimental Results 47
Model Input and Computation 52
Model Results and Interpretation 55
Conclusions 61
Acknowledgments 62
References 63
CHAPTER 4: CONCLUSIONS **67**
VITA **70**

APPENDIX A: Supporting data for Chapter 2
APPENDIX B: Supporting data for Chapter 3
APPENDIX C: Derivation of shrinking sphere model

CHAPTER 1: INTRODUCTION

Over the course of our lives we inhale and retain millions of particles in our lungs from exposures to dusts in both occupational, home, and environmental settings. These dust particles exposures are usually benign, and the dusts merely deposit in our lungs. However, exposures to some types of dusts produce adverse health effects, including respiratory irritation, thickening of alveolar walls, and respiratory cancers. Respirable particles may also contain components that are easily dissolved in the body, releasing doses of toxic agents via the respiratory and digestive systems. Airborne particles come from a wide range of sources, both natural and man-made. For example, weathering produces fine mineral dusts that are readily suspended and inhaled into the lungs. These dusts contain a range of minerals, depending on the source and environment from which the dusts originated. A comprehensive summary of the natural sources of mineral dusts is presented by Klein (1992). Other sources arise from human activities such as mining, smelting, stack emissions, combustion particles from burning fossil fuels, and agricultural activities that expose loose soils to the winds. Particles generated from these anthropogenic sources may be varied in composition, extremely fine grained, and travel great distances through the atmosphere (Pacyna, 1986; Castillo, 1986; Sheridan and Musselman, 1985; Jaspar et al., 1986; Sheridan, 1989; Turpin and Huntzicker, 1991; Kanapilly et al., 1973).

Some mineral dusts and other airborne particulate matter are considered hazardous enough to warrant control of exposures. Exposures to minerals such as erionite are associated with elevated risks of cancer, yet there is no large U.S. population exposed on a regular basis and as a result there are no federally-mandated control limits (Jurinski and Jurinski, 1997). Other airborne mineral and mineral-like particles are subject to regulatory control in the United States through the Occupational Safety and Health Administration (OSHA) and the Environmental Protection Agency (EPA). Specific exposure limits have been promulgated by OSHA for dusts including respirable nuisance dusts, asbestos, and silica. The Environmental Protection Agency has recently imposed controversial regulations under the Clean Air Act

limiting regional concentrations of particulate matter as fine as 2.5 microns in diameter ("PM 2.5"). The EPA opted out of a cost analysis of these new regulations, citing "its longstanding interpretation of the [Clean Air] Act as precluding consideration of costs and similar factors in setting [air quality standards]" (USEPA, 1997). However, estimates of the cost to implement control measures to meet the requirements of the PM 2.5 standard are as high as 55 billion dollars per year (RAP, 1997)! There is still considerable debate on the nature of the exposure to particulate matter in the general population and, more significantly, a lack of consensus on the significance of the health risk posed by exposure to fine particulate matter (Abelson, 1997). These regulations limiting exposure to particulate matter clearly come at great cost to the economy, and should be implemented only on a sound scientific basis.

Evaluating the effects of dust exposures involves a wide range of considerations. The interaction of dust and the body is a complex process and several defense mechanisms are employed by the body to minimize the effects of this exposure. The respiratory system contains specialized scavenger cells that engulf particles and physically transport them from the respiratory system. Some particles, such as chrysotile asbestos, dissolve rapidly under physiological conditions and are cleared from the body through dissolution (Hume and Rimstidt, 1992). Many larger particles are cleared via the mucociliary escalator, a blanket of mucous which is moved upward from the lower respiratory tract by cilia that transport the deposited dust from the airways (Lehnert, 1992). Exposure effects are not limited strictly to the presence of dust in the airway, since complex mixtures of dusts sometimes contain toxic components such as heavy metals. These materials may leach from the particles and be released to the body from the inhaled substrate and distributed throughout the body by the circulatory system. The body attempts to detoxify administered doses through metabolic processes; however metals may accumulate at target organs and cause serious injury if these substances are not cleared. Occasionally, the metabolites themselves present a toxic dose to a target organ.

A general framework from which to evaluate potential adverse effects from dust exposures is presented in Figure 1. Inhalation exposure to respirable dusts leads to the administration of a dose to the individual, which may then lead to an effect. The resulting effects associated with a dose of respirable dust relate to the dust's biopersistence, and the bioavailability of agents released from the inhaled dust. The biopersistence is the total resistance of the particle to removal from the body by physical and chemical means (Jaurand, 1994; Oberdörster et al., 1994). Physical resistance to clearance may result from particle deposition deep in the lung, distant from the mucociliary escalator and resistance to phagocytosis or other sequestering mechanisms. Biodurability, or the ability to resist chemical dissolution, also contributes to the longevity of particles in the lung. Studies characterizing the biopersistence and biodurability of both man-made (e.g. glass and ceramic fibers) and mineral dusts have been performed using *in vivo* and *in vitro* systems (Jaurand, 1994; Oberdörster et al., 1994; Scholze and Conradt, 1987; Kanapilly et al., 1973).

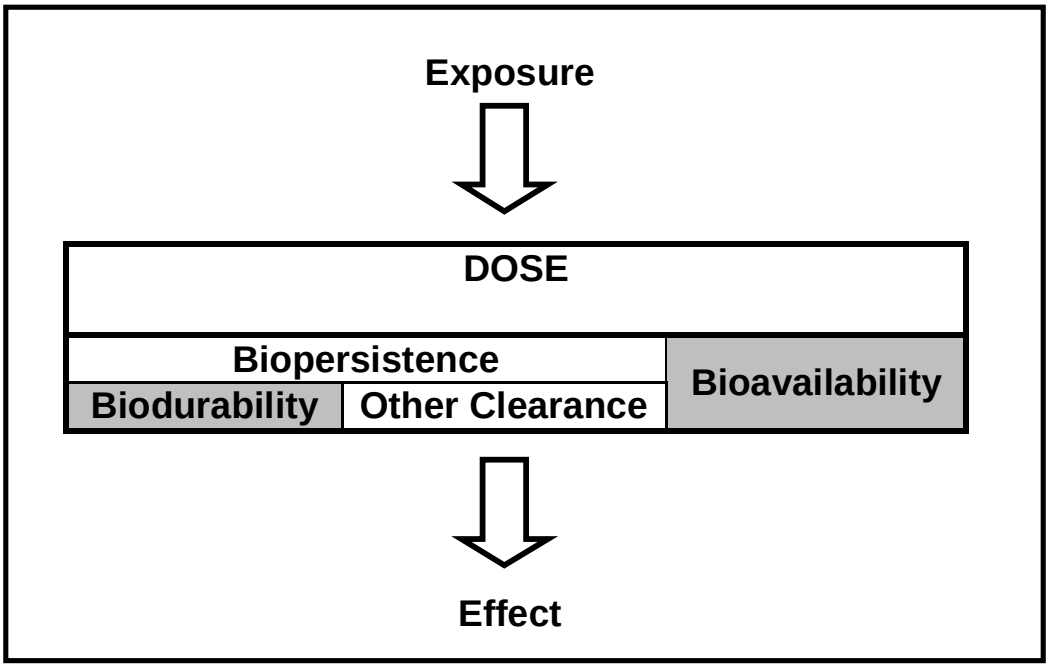

FIGURE 1. This figure shows the relationship between exposure, dose, and effect. The components of a dose characterized by the geochemical investigations discussed in this dissertation are shown in the shaded boxes. The mixed flow reactor was used to describe the biodurability of talc under conditions simulating the lung environment by measuring the release rate of silica, the slowest dissolving component. The bioavailability of arsenic and chromium from coal fly ash was determined by measuring the release rate of these elements under simulated lung and stomach conditions (modified from Oberdörster et al., 1994).

Geochemists have over the past 20 years developed a number of experimental methods to measure the rate of dissolution of mineral and mineral-like substances. Many of these approaches have adapted traditional chemical engineering tools such as batch reactors, plug flow reactors and mixed flow reactors. Rimstidt and Newcomb (1993) have discussed the properties of these reactors and their application to geochemical investigations. Much of the focus of these geochemical investigations has been to characterize the behavior of these substances in the environment, with the goal of evaluating the weathering behavior (Lin and Clemency, 1981, Luce et al., 1972). However, as awareness of the hazards associated with asbestos exposure became general knowledge and regulations were passed limiting workplace exposures in the 1970's, geochemists began adapting their experimental methods to describe behavior of these minerals in the body (Choi and Smith, 1972; Bales and Morgan, 1985; Gronow, 1987). Dissolution experiments designed specifically to estimate particle lifetimes in the body were performed on chrysotile asbestos (Hume and Rimstidt, 1992). Other experiments have been performed to measure the bioavailable fraction of lead from soils to characterize the potential exposure from ingestion by children (Hamel et al., 1998). These dissolution experiments can provide valuable information about the behavior of respired dusts based on studies of the interaction of the dust particles and solvents chosen to simulate body fluids. Selection of appropriate physical and chemical parameters, such as particle size, solvent composition, and reaction temperature yields estimates of particle behavior in the body. Determination of the behavior of key components of a particle under these defined conditions provides information on the fate of particles in the body and the effects of exposure. This information about dust behavior in the body benefits the industrial hygienist who must anticipate the effects of exposure on workers.

The studies presented in this dissertation bridge the disciplines of geochemistry and industrial hygiene by applying geochemical techniques to answer industrial hygiene questions. The next chapter describes the use of a mixed flow reactor to define the biodurability of talc by measuring the rate of release of the slowest dissolving component of the mineral. The release rate of silica was combined with a shrinking

particle model to estimate the lifetime of respirable talc in the lung. The biodurability of talc was compared with the biodurability of other silicates under similar conditions. Chapter three describes the use of a mixed flow reactor experiment to measure the bioavailability of toxic metals from coal fly ash. In this study, the time-release profile of metals from a complex material is described. The time-release profiles of arsenic and chromium from coal fly ash, defined by analysis of effluent from a mixed flow reactor, are used as inputs for a toxicokinetic dose model. The time-release profiles are used to predict the biological response to a coal fly ash exposure. Results predicted from the exposure model are compared with biological monitoring data from a cohort occupationally exposed to coal fly ash.

Studying the behavior of respired particles from the perspective of a geochemist provides a unique view of the response of inhaled particles to the physiological environment. The studies presented in this dissertation show how dust-body interactions can be simulated and highlight the benefits and limitations of a multi-disciplinary approach applying geochemical principles to industrial hygiene problems. These techniques may, in some cases, serve as surrogates for traditional animal testing models for a fraction of the time and cost of animal studies. The final chapter of this document summarizes the relative merits of using a mixed flow reactor to describe the biodurability of respirable mineral particles and the bioavailability of metals dissolved from inhaled dusts.

REFERENCES

Ableson, P. (1997) Editorial: Proposed Air Pollution Standards. Science, v. 277, p. 15.

Bales, R., and Morgan, J. (1985) Dissolution kinetics of chrysotile at pH 7 to 10. Geochimica and Cosmochimica Acta, v. 49, pp. 2281-2288.

Castillo, R. (1986) An analysis of black aerosol found in two winter atlantic coastal snow storms at Whiteface Mountain, New York. Journal of Aerosol Science, v. 17. no. 4, pp 677-684.

Choi, I., and Smith, R. (1972) Kinetic study of dissolution of asbestos fibers in water. Journal of Colloid and Interface Science, v. 40, no. 2, pp. 253-262.

Gronow, J. (1987) The dissolution of asbestos fibers in water. Clay Minerals, v. 22, pp. 21-35.

Hamel, S.G., Buckley, B, and Lioy, P.J. (1998) Bioaccessibility of metals in soils for different liquid to solid ratios in synthetic gastric fluids. Environmental Science and Technology, 32, pp. 358-362.

Hume, A., and Rimstidt J.D. (1992) The biodurability of chrysotile asbestos, American Mineralogist, v. 77, pp 1125-1128.

Jaspar, S. M., Brachaczek, W.W., Gorse, R.A., Jr., Norbeck, J.M., and Pierson, W.R. (1986) The contribution of elemental carbon to the optical properties of rural atmospheric aerosols. Atmospheric Environment, v. 20, no. 6, pp. 1281-1289.

Jaurand, M. (1994) In Vitro assessment of biopersistence using mammalian cell systems. Environmental Health Perspectives v. 102(supplement 5) pp. 55-59.

Jurinski, J, and Jurinski, N. (1997) A proposed control limit for exposure to airborne erionite fibers. Applied Occupational and Environmental Hygiene, v. 12, no. 6. pp 429-434.

Lin, F., and Clemency, C.V. (1981) The dissolution kinetics of brucite, antigorite, talc, and phlogopite at room temperature and pressure. American Mineralogist, 66, 801-806.

Lehnert, B. (1992) Defense mechanisms and particle-cell interactions. in Health Effects of Mineral Dusts. George Guthrie and Brooke Mossman, Eds. Mineralogical Society of America. 427-469.

Luce, R.W., Bartlett, R.W. and Parks, G.A. (1972) Dissolution kinetics of magnesium silicates. Geochimica and Cosmochimica Acta, 36, pp 35-50.

Kanapilly, G.M., Raabe, O.G., Goh, C.H.T., and Chimenti, R.A. (1973) Measurement of *in vitro* dissolution of aerosol particles for comparison to *in vivo* dissolution in the lower respiratory tract after inhalation. Health Physics, v. 24, pp. 497-507.

Klein, C. (1993) Rocks, minerals and a dusty world. in Health Effects of Mineral Dusts, George D. Guthrie and Brooke T. Mossman, eds. American Mineralogical Society Reviews in Mineralogy v. 28. pp 7-60.

Oberdörster, G., Ferin, J., and Lehnert, B. (1994) Correlation between particle size, in vivo particle persistence, and lung injury. Environmental Health Perspectives, v. 102 (supplement 5) pp. 173-179.

Pacyna, J.M (1986) Emission factors of atmospheric elements. in Toxic Metals in the Atmosphere, Jerome O. Nriagu and Cliff I. Davidson, eds. John Wiley and Sons, New York, pp, 1-32.

RAP (1997) Comments on the Proposed National Air Quality Standards for Ozone and Particulate Matter, Regulatory Analysis Program, Center for Study of Public Choice, George Mason University, March 12, 1997, p. 2.

Rimstidt, J.D., and Newcomb, W (1993) Measurement and analysis of rate data: The rate of reaction of ferric iron with pyrite. Geochimica and Cosmochimica Acta, 57, 1919-1934.

Scholze, H., and Conradt, R. (1987), An *in vitro* study of the chemical durability of siliceous fibres. Annals of Occupational Hygiene, v. 31, no 4B, pp. 683-692.

Sheridan, P. (1989) Characterization of size segregated particles collected over Alaska and the Canadian High Arctic, AGASP-II flights 204-206. Atmospheric Environment, v. 23, no. 11, pp. 2371-2386.

Sheridan, P.J., and Musselman, I.H. (1985), Characterization of aircraft-collected particles present in arctic aerosol; Alaskan Arctic, Spring 1983. Atmospheric Environment, v. 19, no. 12, pp. 2159-2166.

Turpin, B. J., and Huntzicker, J.J. (1991) Secondary formation of organic aerosol in the Los Angeles Basin: A descriptive analysis of organic and elemental carbon concentrations. Atmospheric Environment. v. 25A, no. 2, pp. 207-215.

USEPA (1997) National Ambient Air Quality Standards for Particulate Matter, Final Rule (40 CFR Part 50) Federal Register: July 18, 1997 (Volume 62, Number 138)Page 38651-38701.

CHAPTER 2: BIODURABILITY OF TALC

ABSTRACT

Dissolution rates of a well-characterized sample of powdered talc were measured in solvents that mimic fluids found in the human lung. These experiments found that talc dissolution rates were the same for pH controlled aqueous solvents, phosphate buffered saline solution, and modified Gamble's solutions. They showed that variation of solvent chemistry, including the addition of organic chelators and proteins at intercellular fluid concentrations, does not markedly affect the measured dissolution rate of talc at 37°C and the data further indicate that the dissolution mechanism for talc in aqueous solutions is independent of pH over a range of pH from 2 to 8. The dissolution rate at 37°C, determined by measuring the silicon release rate per unit surface area of talc in a mixed-flow reactor system, is 1.4 (± 1.0) x 10^{-11} mol Si/(m^2 - sec). Application of a geometric shrinking particle model using this dissolution rate results in an estimated lifetime (upper limit) of approximately 8 years for a 1 micron talc particle under pulmonary conditions. Talc dissolves considerably faster than quartz, but slower than chrysotile and olivine in the body. These data can be used to place constraints on the role of particle dissolution in the disease models associated with airborne respirable particles.

INTRODUCTION

The recent focus on the behavior and control of inhaled mineral particles by the medical and regulatory communities presents geochemists an opportunity to extend principles traditionally employed in characterizing the dissolution of minerals into the new field of biologically-based dissolution studies. Adaptation of traditional dissolution rate studies to mimic the physical and chemical conditions encountered in the lungs allows geochemists to estimate biodurability in the lung through calculation of residence times based on the dissolution clearance mechanism. Mineral dusts are pervasive in our environment and we are continuously exposed to them on a daily basis. Mechanical and chemical weathering processes produce readily suspended dusts, which may then be taken up into the lungs. The respiratory exposure to specific mineral dusts has long been known to cause adverse heath effects, including scarring and thickening of the tissues of the lung, and the development of cancer. For instance, exposures to airborne asbestos minerals are known to cause mesothelioma, lung cancer, other cancers, and other lung diseases, such as asbestosis. Similarly, exposure to elevated concentrations of quartz can produce silicosis, and occupational exposures to high concentrations of relatively "pure" airborne talc dusts have been linked to talcosis, a relatively benign lung pneumoconiosis (Gamble, 1986). The effects of exposure are considered severe enough that exposures to dusts, including mineral dusts, are regulated in the workplace. The United States Environmental Protection Agency also regulates fine airborne particulate matter, which includes mineral dusts, through Clean Air Act regulations.

Talc is used in a range of everyday products from cosmetics to paper and its extensive use results in exposures to a large segment of the population in both the work place and in the home. Talc is so widely used that exposures extend from infancy through old age. This widespread use has resulted in a large potential for exposure to the mineral through dermal and airborne routes.

The physical characteristics of the inhaled particles determine where particles will deposit in the lung. Particle dimensions and surface properties, as well as the velocity of the air stream in the respiratory

system determine the depth to which particles may penetrate the lung. In general, particles with aerodynamic diameters greater than approximately 10 microns impact in the upper reaches of the respiratory tract and are rapidly moved up the bronchioles by specially adapted ciliated cells (the mucociliary escalator) which sweep the particles towards the throat. These particles are then cleared and expectorated or swallowed. Particles with equivalent diameters of approximately 1-2 microns are most likely to penetrate deeply to the alveolar regions of the lung (Glenn and Craft, 1986). The body's natural clearance processes are not as efficient in the deep lung, and these particles may persist. These very fine particles are of the most concern because their presence in these tissues can result in scarring of the alveolar walls which results in reduction of the ability to exchange gasses across the alveolar membrane.

One factor controlling the tendency of a given particle to cause a disease must be related, in part, to the residence time of the particle in the pulmonary environment. Mineral dusts are cleared from the lung by several different mechanisms, including exhalation of suspended particles, sequestering of particles by specialized cells (macrophages), relocation via the mucocilliary escalator and via the lymphatic system, *in situ* dissolution, or a combination of these mechanisms (Lehnert, 1992). One of the factors controlling the residence time is a particle's biodurability, or its resistance to chemical dissolution. We wish to distinguish the term "biodurability" from "biopersistence" which we define as a particle's total resistance to all clearance mechanisms. The biodurability of mineral dusts may then be a factor in the tendency for a dust exposure to result in disease. However, to describe adequately the dissolution behavior of minerals in the human lung, it seems reasonable that the solvent solutions must reflect the biochemical composition of the lung fluids. The presence of certain biological compounds, including organic chelators such as sodium citrate has been shown to increase the dissolution rate of cations from minerals (Lund and Aust, 1990, Werner, et al., 1995).

Previous Studies

Dissolution studies of magnesium silicates have been performed under a range of conditions, yet few have been designed to measure dissolution behavior under physiological conditions. Lin and Clemency (1981) studied the dissolution kinetics of a suite of magnesium silicates, including talc, at room temperature and pressure using a batch reactor. Talc dissolved incongruently in the experiments. Incongruent dissolution of a suite of magnesium silicates (serpentine, forsterite, and enstatite) was also noted by Luce et al. (1972). Hume and Rimstidt (1992) measured the dissolution rate of chrysotile at 37°C, and determined that a 1 micron fiber would have an expected lifetime of 9 months in the lung, based on a silica release rate of approximately 6×10^{-10} mol Si/m^2 sec from a shrinking cylinder model.

Gamble (1942) presented a text in which the compositions of physiological fluids were described. This work has served as a basis for a number of experimental derivations for human intercellular fluid, including the experimental solvents used by Scholze and Conradt (1987), and the solutions of Kanapilly, et al. (1973). Experimental derivations of fluids based on Gamble's description have typically included protein free solutions mimicking anionic and cationic compositions of the intercellular or serous fluids.

This study investigated the estimated clearance rate of talc using a mixed flow reactor method modified to simulate lung conditions. Specifically, the experiments were conducted at a fixed temperature of 37°C. Preliminary work indicated that the dissolution rate was independent of pH over a pH range of 2-8 so that precise buffering of the reactor to a physiological pH of 7.4-7.5 was unnecessary. Nevertheless, several runs were buffered at a pH of approximately 7.5, using a phosphate-buffered saline solution. The modified Gamble's solutions were buffered to a pH of approximately 7.8.

METHODS

Talc Sample

Five kilograms of Fisher Scientific Talcum (Lot #920194) were obtained for the experiments and used as received from the manufacturer. A sample of the talc prepared following Asbestos Hazard Emergency Response Act (AHERA) methods (40 CFR Part 763, Appendix A to Subpart E) was analyzed using transmission electron microscopy (TEM). TEM observation of the sample showed that the material was relatively homogeneous in composition. Trace (<1%) quantities of quartz, and an iron-magnesium bearing aluminosilicate were observed. Particle size distribution data reported by the manufacturer for the product are listed in Table 1.

TABLE 1. The distribution of particle sizes for the talc sample used in these experiments.

Size Split	Cumulative Weight %
> 30 μm	4.3
> 20 μm	8.6
> 10 μm	72
> 5 μm	74
> 4 μm	79
> 3 μm	89
> 2 μm	94
> 1 μm	>99

Surface Area Analysis

The specific surface area of the talc was measured using a Quantachrome Surface Area Analyzer following the method of Brunauer et al. (1938). Nitrogen was used as the adsorbate gas. The samples were outgassed at 125° C under a vacuum for approximately 2 hours prior to analysis. The talc used for the experiments had a specific surface area of 6.01 m^2/g.

Solvent Preparation

A series of experiments were performed in solvents of increasing physiological relevance. First, the dissolution rate of talc in deionized water adjusted to pH values of 2, 4, and 7.4 using hydrochloric acid or sodium hydroxide was measured. Then the dissolution rates were measured with a phosphate buffered saline solution with a pH fixed at approximately 7.4. The composition of the phosphate buffered saline solution is shown in Table 2. Finally, the dissolution rate of talc was measured in two types of "Gamble's" solutions. One solution was prepared following the formulation of Scholze and Conradt (1987). An additional solution was based on this same composition but included protiene in concentrations comparable to those found in the intercellular fluid description of Gamble (1942). Ova albumen was chosen as the protein surrogate since it is the most abundant protein in serum plasma (Lentner, 1984). The composition of the Gamble's solutions used in our experiments is listed in Table 2.

TABLE 2. Solvent Composition

Component	Concentration (mg/L)
Phosphate Buffered Saline	
KCl	212
NaCl	6,400
KH_2PO_4	255
Na_2HPO_4	179
Gamble's Solution	
$MgCl_2 \bullet 6H_2O$	212
NaCl	6,400
$CaCl_2 \bullet 2H_2O$	255
$Na_2SO_4 \bullet 10H_2O$	179
Na_2HPO_4	148
$NaHCO_3$	2,700
Na_2 tartrate$\bullet 2H_2O$	180
Na_3 citrate$\bullet 2H_2O$	153
Na lactate (60% w/w)	290
Glycine	118
Na pyruvate	172
ova albumen (when used)	445

Mixed Flow Reactor Method

Measurements of dissolution rates of talc at 37°C were performed using a mixed flow reactor following procedures modified from Rimstidt and Newcomb (1993). Figure 1 shows a schematic layout of the basic design of the experimental system in which a 125 mL reaction vessel constructed of acrylic plastic was used. The sample was agitated using a bar magnet rotated using an overhead magnetic stirrer. Agitation of the high-viscosity protein-rich experiments was accomplished using a wrist-action shaker because the stir bar was unable to keep the talc suspended in the reactor using an overhead stirrer. At the beginning of each experiment, a known weight of solid material (usually 5.00 grams) was loaded into the reactor. Solvent solutions were pumped through the system using a peristaltic pump at flow rates ranging from 0.5 to 1 mL/min. The flow rate was determined at several times through the individual experimental runs by measuring the time required to collect a known volume of effluent. Flow rates of protein rich solutions were lower due to the higher viscosity, and averaged approximately 0.2 mL/min. The pH data were collected at defined times (typically every 15 minutes) using a serial printer interfaced to an in-line Beckman phi 72 pH meter equipped with a Beckman #39537 electrode.

After the system had reached steady state, as indicated by a constant effluent pH, 30 mL of effluent were collected, usually sometime after two hours of run time. Most experiments were run for longer periods of time. The effluent was collected into acid-washed, triply (deionized water) rinsed 30 mL Nalgene® bottles. The pH and the flow rate of the effluent were recorded at the time of sample collection. All samples were acidified with 1 mL of nitric acid. Stored samples were refrigerated prior to analysis.

Silica Analysis

The silica and magnesium concentrations of the samples were determined using Inductively Coupled Plasma (ICP) analyses. Silica concentrations were measured by integration of the Si 251.611 nm peak. Concentration measurements were referenced to standard solutions prepared from a 1000 ppm Fisher Scientific Si reference standard. The analytical limit of detection was 0.078 ppm and the relative standard

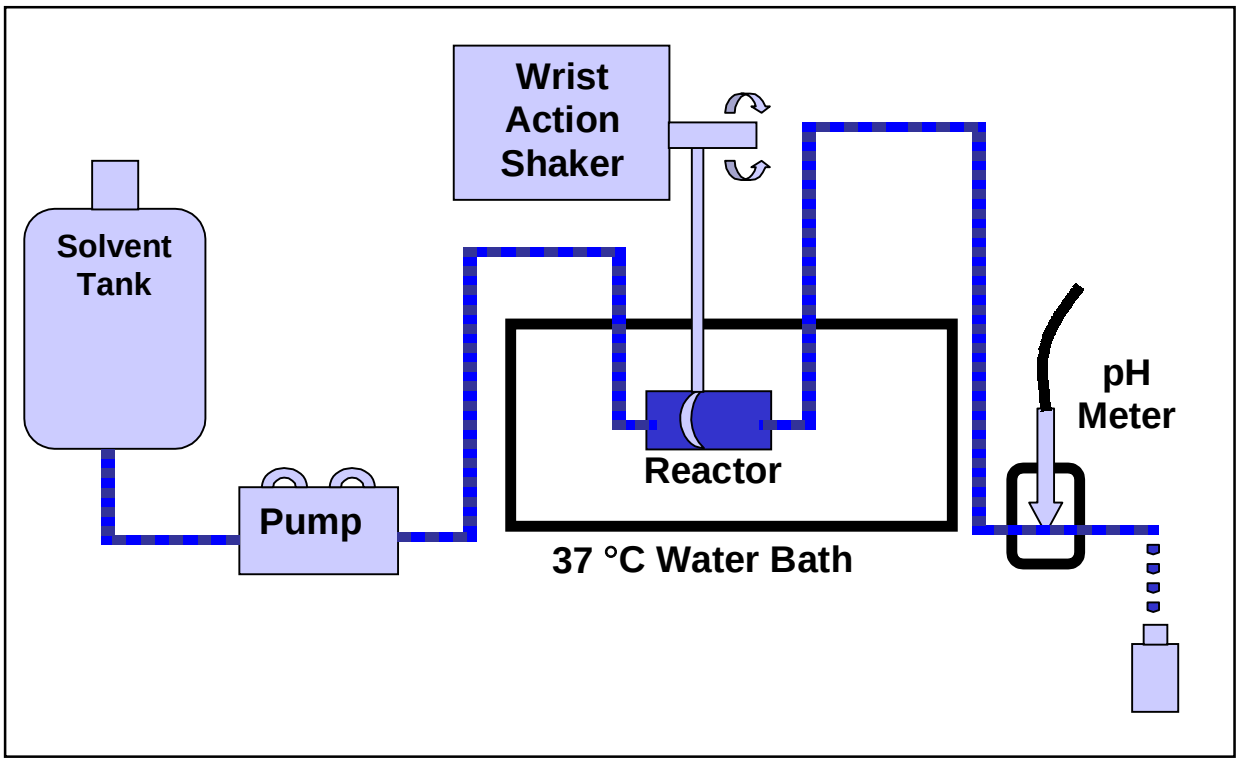

FIGURE 1. Schematic of mixed flow reactor design. Solvent was pumped through an acrylic plastic reaction vessel submerged in a 37°C water bath. The wrist action shaker was used for protein-containing samples. A magnetic overhead stirrer was used for other samples.

deviation was 3.9%. The protein-free samples were analyzed without dilution. Protein was precipitated from albumen-containing samples using nitric acid. These samples were centrifuged at 5,000 g, and then filtered through Whatman #2 qualitative filter paper. The recovered supernatant was aspirated directly into the ICP for analysis. Solvent blanks did not contain detectable concentrations of silica. Magnesium concentrations were measured and are reported in Appendix A. The high background concentration of magnesium in the Gamble's solution was far in excess of the contribution from the dissolution from talc.

ANALYTICAL RESULTS

The type of experiment, weight of solids, and measured flow rate for each sample are included in Table 3. The measured silica concentration and the pH of the solution at the time of collection are also tabulated. A normalized rate constant, k (mol Si/m^2 sec), was calculated for each sample (Table 3) using the Si

concentration, reactor flow rate, sample weight, and the sample specific surface area using the following equation:

$$k(\frac{moleSi}{M^2 \bullet \sec}) = \frac{flowrate(\frac{kg}{\sec}) \bullet Si(\frac{mole}{kg})}{SampleWeight(g) \bullet SpecificSurfaceArea(\frac{M^2}{g})}$$

The results in Table 3 have been grouped by solvent type, and the rate constants are plotted against the pH of the sample in Figure 2. The results indicate the average rate of silica release from talc is 1.4 (± 1.0) x 10^{-11} mole Si/m^2 sec (n=49, 1 σ error).

TABLE 3. Sample characteristics for samples taken at steady state. PBS – Phosphate Buffered Saline, Gamble's – Gamble's Solution, Protein – Gamble's solution plus albumen (Table 2).

Sample #	Weight (g)	Flow Rate (mL/min)	pH	Si (ppm)	Si (mole/m2sec)	log (Si mole/m2 sec)
pH 4						
41117A	5	0.88	8.8	0.83	1.44×10^{-11}	-10.8
41118A	5	0.51	9.2	1.4	1.41×10^{-11}	-10.9
41121A	5	0.88	9.1	0.93	1.62×10^{-11}	-10.8
41122A	5	0.57	9.0	0.94	1.06×10^{-11}	-11.0
41123A	5	0.67	8.7	0.61	8.07×10^{-12}	-11.1
41125A	5	1.1	8.7	0.48	1.04×10^{-11}	-11.0
41125B	5	1.1	8.0	0.49	1.06×10^{-11}	-11.0
41128A	3.97	1.03	6.8	0.39	9.99×10^{-12}	-11.0
41128B	3.97	1.03	6.0	0.26	6.66×10^{-12}	-11.2
41130A	4.6	0.95	6.3	0.56	1.14×10^{-11}	-10.9
41130B	4.6	0.95	5.0	0.31	6.32×10^{-12}	-11.2
41130C	4.6	0.95	4.1	0.29	5.91×10^{-12}	-11.2
pH 7						
41202A	5	0.88	8.5	0.80	1.39×10^{-11}	-10.9
41202B	5	0.88	7.7	0.30	5.21×10^{-12}	-11.3
41219A	5	0.96	9.0	0.43	8.15×10^{-12}	-11.1
41219B	5	0.96	8.5	1.1	2.08×10^{-11}	-10.7
PBS						
41220A	5	1.11	8.1	0.88	1.93×10^{-11}	-10.7
41220B	5	1.11	8.1	0.62	1.36×10^{-11}	-10.9
41221A	5	1.1	7.4	0.64	1.39×10^{-11}	-10.9
41221B	5	1.1	7.4	0.41	8.9×10^{-12}	-11.1
41223A	5	1.1	8.0	0.38	8.25×10^{-12}	-11.1

Sample #	Weight (g)	Flow Rate (mL/min)	pH	Si (ppm)	Si (mole/m2sec)	log (Si mole/m2 sec)
41227A	5	1.08	7.5	2.8	5.97×10^{-11}	-10.2
41227B	5	1.08	7.4	0.60	1.28×10^{-11}	-10.9
41228A	5	0.7	7.5	3.5	4.84×10^{-11}	-10.3
41228B	5	0.7	7.4	1.8	2.49×10^{-11}	-10.6
41228C	5	0.7	7.3	1.2	1.66×10^{-11}	-10.8
41229A	3.97	1.05	7.4	0.24	6.26×10^{-12}	-11.2
41229B	3.97	1.05	7.4	0.23	6.00×10^{-12}	-11.2
pH 2						
50501A	5	0.98	1.5	0.76	1.47×10^{-11}	-10.8
50501B	5	0.98	1.5	0.72	1.39×10^{-11}	-10.9
50502A	5	0.77	1.9	2.2	3.34×10^{-11}	-10.5
50502B	5	0.77	1.8	1.1	1.67×10^{-11}	-10.8
50503A	4.69	1.03	1.9	0.56	1.24×10^{-11}	-10.9
50503B	4.69	1.03	1.8	0.46	9.97×10^{-12}	-11.0
50504A	5	0.96	1.9	1.5	2.84×10^{-11}	-10.5
50504B	5	0.96	1.8	0.79	1.50×10^{-11}	-10.8
Gamble's						
50703A	5	0.99	8.1	0.72	1.41×10^{-11}	-10.8
50703B	5	0.99	8.1	0.53	1.04×10^{-11}	-11.0
50704A	5	0.66	5.2	1.2	1.56×10^{-11}	-10.8
50705A	5	0.95	7.7	1.1	2.06×10^{-11}	-10.7
50705B	5	0.95	7.7	0.38	7.13×10^{-12}	-11.2
50706A	4.02	0.99	7.7	0.33	8.02×10^{-12}	-11.1
50706B	4.02	0.99	7.7	0.15	3.65×10^{-12}	-11.4
Protein						
61205-1	5	0.30	7.5	2.9	1.74×10^{-11}	-10.8
61205-2	5	0.25	7.5	2.4	1.19×10^{-11}	-10.9
61206-1	5	0.18	7.7	2.0	7.18×10^{-12}	-11.1
61206-2	5	0.16	7.6	2.0	6.19×10^{-12}	-11.2
61207-1	5	0.25	7.8	2.2	1.07×10^{-11}	-11.0
61207-2	5	0.12	7.7	2.3	5.49×10^{-12}	-11.3

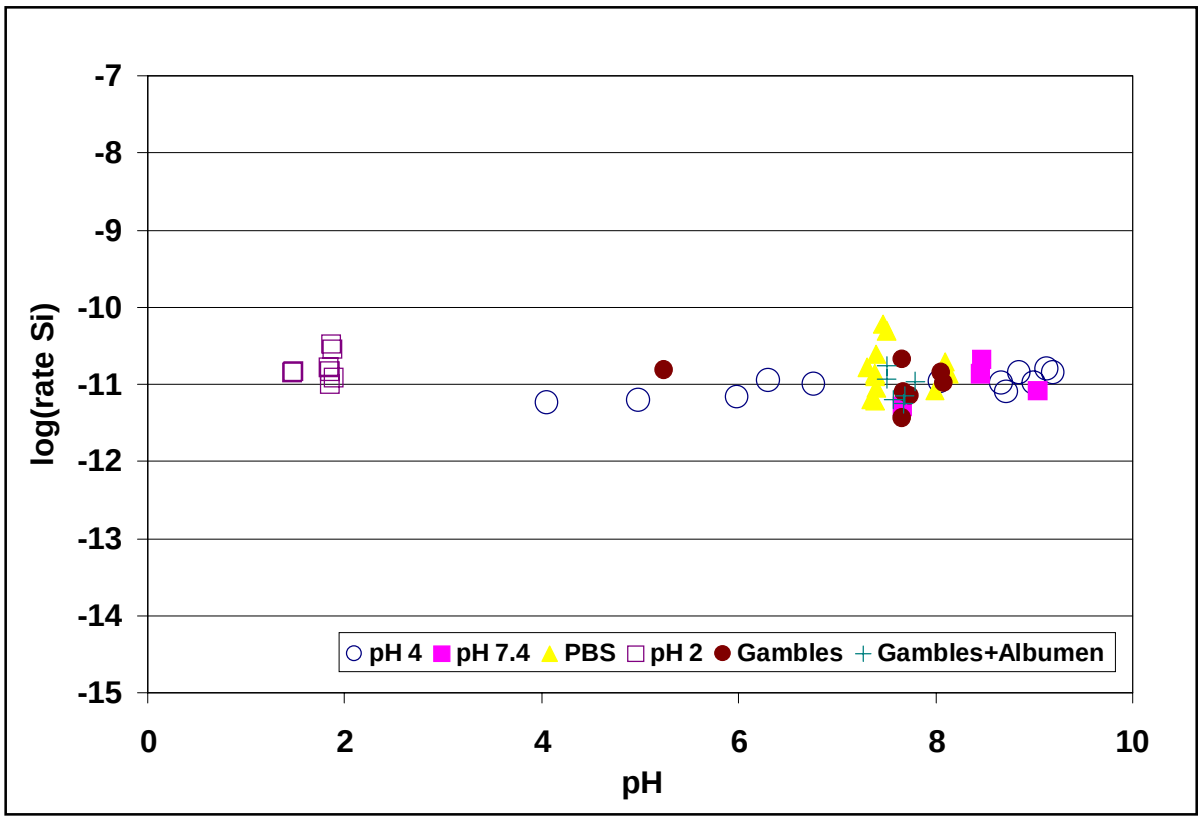

FIGURE 2 . Log k (mole Si / m^2 sec) versus pH of sample effluent. The data are plotted by solvent type. The rate constant for the release of silica from talc is independent of pH and is 1.4 (±1.0) mole Si / m^2 sec.

DISCUSSION

Silicates are used extensively in industry. Olivine is processed as a source of magnesium and olivine sands are used in high temperature foundry operations and as a substitute for quartz sand. The number of workers exposed regularly to olivine is, however, relatively small. There have been no reports of occupational respiratory disease associated with exposure to olivine, although there is no epidemiological data describing the effects of exposure (Gamble, 1985). Chrysotile asbestos is considered a human carcinogen, and regulated as such in the U.S. workplace (Stayner, et al., 1996, USDOL, 1994). Historically, chrysotile was used extensively in the United States. Chrysotile was incorporated into a wide range of commercial products due to its thermal stability and tensile strength, including thermal systems insulation, vehicle brake linings, transite siding, vinyl floor tile, and decorative or thermal architectural finishes. Exposures to chrysotile were associated with the processing of the mineral and the

manufacturing and application of asbestos containing products. Exposures to crystalline silica (mostly quartz) are widespread, both from the workplace and the environment. Exposure to crystalline silica in the workplace has been linked to silicosis, a progressive pneumoconiosis. Debate on the role of crystalline silica in the development of cancer in exposed populations continues, but it is unlikely that significant cancer risk is associated with exposures to crystalline silica at current occupational exposure control limits (McDonald, 1995). Talc is used extensively in industry and is incorporated into a wide range of products including paints, coatings, cosmetics, pharmaceuticals, and as coatings on paper. As a result, the cohort of potentially exposed workers is much larger than the population of olivine-exposed workers. Chronic exposures to high concentrations of talc have been associated with development of talcosis, a benign pneumoconiosis (Gamble, 1985). Confounding coincident exposures to crystalline silica and amphibole asbestos have been noted.

The silica dissolution rate measured in this study can be used to determine the dissolution rate of talc. The congruent dissolution reaction for talc is $Mg_3Si_4O_{10}(OH)_2 + 6H^+ + 4H_2O = 3Mg^{2+} + 4H_4SiO_4$ (Lin and Clemency, 1981). However, our experiments, as well as those of Lin and Clemency (1981) showed talc dissolves incongruently so that the rate of release of magnesium always exceeds the release rate of silica. This results in the formation of a silica-rich surface on the mineral grains. Therefore, the rate-limiting step in the destruction of the talc particles is the release of silica. Figure 2 shows that the release rate of silica from the talc surface is independent of pH over a pH range of 2-8. This is reasonable because the silica dissolution reaction does not consume or produce H^+, since:

$$(SiO_2)_n + 2nH2O = nH_4SiO_4$$

Furthermore, Figure 2 shows that the rate of dissolution is independent of the solvent chemistry (i.e. pH, buffering capacity, addition of chelators, and addition of protein).

The rate constant for the release of silica can be used to estimate the lifetime of respirable talc particles in the body. The rate limiting step in the destruction of a mineral grain is determined by the rate of release

of the slowest dissolving component (Hume and Rimstidt, 1992). Estimates of particle lifetime were obtained by applying the measured silica dissolution rate to a geometric shrinking particle model. Particle geometry is relatively unimportant in the determination of the biodurability, since the variation in the geometry of shrinking particles (assuming dissolution from major surfaces) affects dissolution estimates by no more that about a factor of three. The major factor limiting the dissolution of magnesium silicates is the release rate of silica from the mineral surface, which may vary by several orders of magnitude.

For talc, the estimate of particle longevity was modeled using a "shrinking sphere" geometry. This approach was similar to that used by Hume and Rimstidt (1992) in their discussion of chrysotile dissolution. The shrinking sphere model assumes dissolution occurs evenly across the surface of the sphere. The time to dissolve the sphere is defined by the diameter of the particle, and is determined by the following relationship, which is derived in Appendix C.

$$t = \frac{d}{2kV_m}$$

where t is time (sec), d is the particle diameter (m), V_m is the molar volume (m^3/mole) and k is the rate constant (mol/m^2 sec). Application of the shrinking sphere model with the measured silica dissolution rate indicated an estimated lifetime of 8 years for a 1 μm talc particle.

The approach used to estimate the lifetime of talc in the body may be extended to other mineral dusts, provided that the rate constants for their dissolution are available. Established rate constants for selected silica phases and magnesium silicates are shown in Table 4, which lists silica release rate constants at 37°C (body temperature) and molar volumes for forsterite, chrysotile and quartz, for comparison with the talc dissolution results of this investigation. Rate data for the dissolution of silica from chrysotile asbestos were obtained from Hume and Rimstidt (1992). Hume and Rimstidt established the silica

release rate from chrysotile asbestos at 37°C over a pH range of 2 to 6. Incongruent dissolution of chrysotile was noted, with magnesium release to solution in excess of its stochiometric amount in chrysotile. A general rate law for silica release from forsterite was developed by Rosso and Rimstidt (in preparation). The release of silica from olivine is dependent on both pH and temperature and is 7.6×10^{-11} mol Si/m^2 sec at 37°C and pH 7. The rate of silica release from quartz at 37°C is 1.4×10^{-13} mol Si/m^2 sec (Rimstidt and Barnes, 1980). The data listed in Table 4 were used with the shrinking sphere model to calculate the curves relating particle size to estimated particle lifetime (Figure 3). The results indicate the wide range of biodurability associated with respirable sized mineral particles. Estimated particle lifetimes do not correlate with the Si:OH ratio of the minerals investigated. Similarly, calculated particle lifetimes based on silica release rates do not correlate with the polymerization of the silicate framework. For example, the estimated lifetime for a one micron diameter olivine sphere is greater than at that of a one micron diameter chrysotile sphere by a factor of approximately 6. Most of the difference in estimated lifetime results from the slower release of silica from the mineral surface.

TABLE 4. Mineral Lifetime Estimates for a 1 micron particle

Mineral	k (mole Si/m^2sec)	Molar Volume, V_m, (m^3/mole)	Time to Dissolve 1 μm particle
Talc	1.4×10^{-11}	1.4×10^{-4}	8 years
Chrysotile	5.9×10^{-10}	1.1×10^{-4}	7 months
Olivine	7.6×10^{-11}	4.4×10^{-5}	4.8 years
Quartz	1.4×10^{-13}	2.2×10^{-5}	5000 years

Molar volume data from Robie *et al.* (1979)
Chrysotile rate constant from Hume and Rimstidt (1992)
Olivine rate constant for pH 7, 37°C from Rosso and Rimstidt (in preparation)
Quartz rate constant for 37°C from Rimstidt and Barnes (1980)

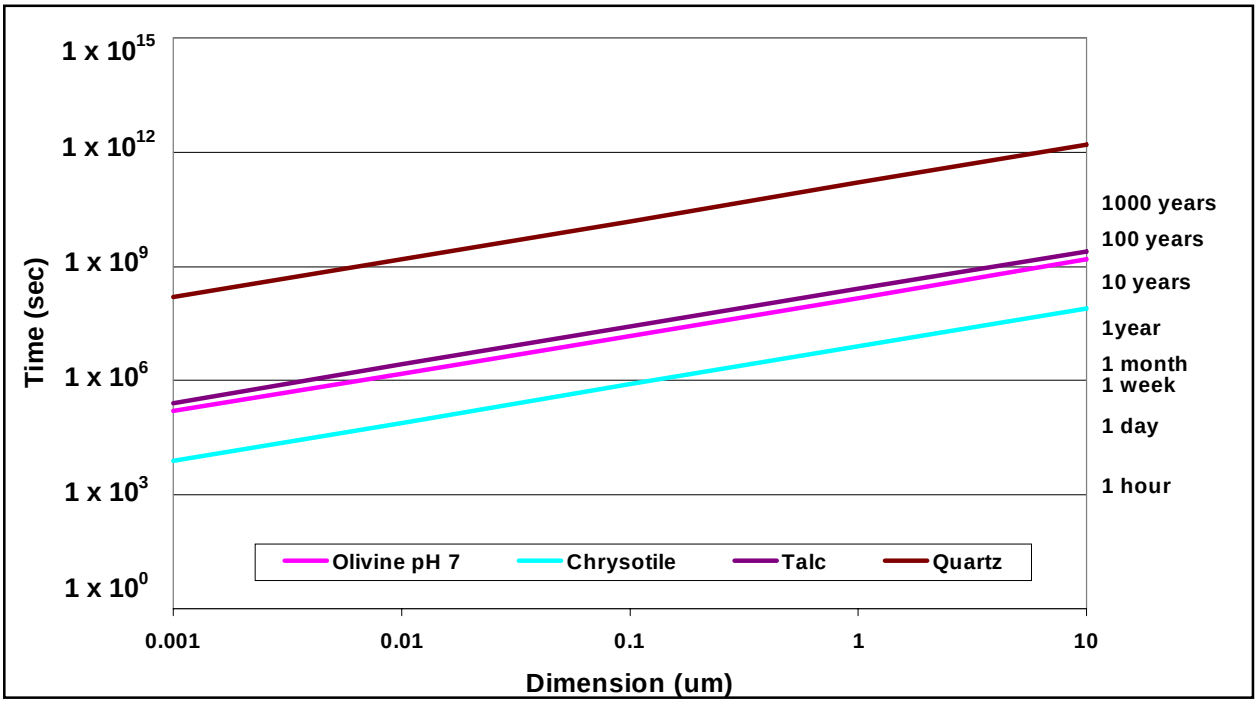

FIGURE 3. Particle dimension (μm) versus time (sec) for dissolution for talc, chrysotile, olivine and quartz. The line labeled quartz was calculated using the dissolution rate constant of Rimstidt and Barnes (1980). The olivine line was calculated with the rate constant of Rosso and Rimstidt (in preparation). The chrysotile line was calculated with the rate constant of Hume and Rimstidt (1992).

Strict application of the geometric shrinking particle model may overestimate the lifetime of the talc particles. The geometric models assume that dissolution occurs evenly across the major surfaces of the geometric solid, and that one major dimension governs the particle lifetime. Talc likely does not dissolve evenly across its basal surface. Turpault and Trotignon (1994) noted that dissolution of biotite occurred primarily along the lateral surface of the crystals. If dissolution is restricted to the edges of the talc grains as opposed to the total measured surface area, the calculated silica release rate would increase in proportion to the decrease in surface area since the surface area is a factor in the denominator of the rate calculation. For instance, a 10-fold reduction in the modeled active dissolution surface would result in a corresponding 10-fold increase in the calculated silica release rate. An increase in the calculated silica release rate would result in decreased estimates of particle longevity in the body from application of the shrinking particle model, since this would indicate that the grains are dissolving more rapidly. Since our

surface area measurements are of the total surface area of the talc sample, the lifetime estimate presented here should be considered a maximum estimate of particle longevity.

These results suggest there is no direct correlation between the dissolution rate of a particle under physiological conditions, and its potential to cause disease. Chrysotile dissolves quickly under physiological conditions, yet is considered a known human carcinogen and has been linked with development of fibrotic lung disease in elevated exposure conditions. Crystalline quartz dissolves very slowly in the body, and is associated with progressive lung disease related to both acute and chronic exposure to high silica dust concentrations. Making a clear correlation between crystalline silica exposure and development of respiratory cancer is problematic. Magnesium silicates with intermediate biodurability appear relatively innocuous.

The lack of direct correspondence between particle dissolution rates under physiological conditions and disease causing potential indicates that additional factors must be considered when evaluating the potential of a mineral dust to cause disease upon exposure. Particle morphology has been implicated in the carcinogenic potential of mineral dusts. Stanton et al. (1981) proposed that the shape of a fiber is the main factor in determining its carcinogenicity, however the implantation methods utilized by Stanton and co-workers may have increased the incidence likelihood of tumor production limiting interpretation of the data (Nolan and Langer, 1992). The generation of free radicals, which has been tied to interactions between mineral surfaces and the physiological environment, has been linked to the disease process (Mossman, 1992; Driscoll, 1992; Werner et al., 1995). The surface properties of the minerals, and the effects of interactions between these surfaces and the physiological environment, likely play an important role in the disease process. Indirectly, particulate matter lodged in the respiratory system may affect the disease process, since the body deploys several defense mechanisms in response to the deposition of particles in the pulmonary system. These include mobilization of alveolar macrophages and other scavenger cells, which respond to the presence of foreign material in the body. The presence of foreign

particles can result in the production of chemoattractant factors which serve to mobilize the body's immune response (Driscoll, 1992; Lehnert, 1992). Several of the compounds released from activation of the macrophages have been linked to the development of fibrosis in the lung (see Driscoll, 1992 and Lehnert, 1992 for discussion of the pulmonary system response to inhaled particles). The presence of particulate matter in the airway, serving as a local stimulant to the inflammatory response, can cause damage to the cells of the pulmonary system. In this manner, the continued presence of the particulate matter should affect the disease development process.

CONCLUSIONS

The mixed flow reactor method described here is straightforward to implement and interpret and provides an effective way to simulate the dissolution behavior of minerals in the pulmonary environment. The dissolution rate of talc is 1.4 (±1.0) mol Si /m^2 sec and the rate is independent of pH and solvent chemistry, including the presence of organic chelators and proteins at physiological concentrations. This dissolution rate can be used with a shrinking sphere model to estimate a lifetime of 8 years for a 1 μm talc particle. The dissolution rates of silicates depend largely on the rate of silica release from the surface of the mineral grains. The relative biodurability of selected silicates is quartz>>talc>olivine>chrysotile. Mineral biodurability does not seem to be a strong factor in the development of pulmonary disease, since biodurability does not appear to correlate with the disease causing potential of mineral dust exposures.

ACKNOWLEDGMENTS

ICP support was provided through the industrial hygiene laboratory of American Medical Laboratories (AML), Inc., of Chantilly, Virginia, and through HP Environmental Laboratories, Inc. of Herndon, Virginia. The assistance of Bryan Mason (AML) and Dr. Hugh Granger (HP) with ICP analysis is gratefully acknowledged.

REFERENCES

Brunauer, S. Emmett, P. H., and Teller, E. (1938). Adsorption of gases in multimolecular layers. Journal of the American Chemical Society, 60, 309-324.

Driscoll, K.E. (1992) In vitro evaluation of mineral cytotoxicity and inflammatory activity. in Health Effects of Mineral Dusts. George Guthrie and Brooke Mossman, Eds. Mineralogical Society of America. 489-511.

Gamble, James L., (1942) Chemical Anatomy, Physiology, and Pathology of Extracellular Fluid: A Lecture Syllabus. 6th Ed. Harvard University Press, Cambridge, Massachusetts, 164 p.

Gamble, John F. (1986) Silicate Pneumoconiosis. in Occupational Respiratory Diseases, James A. Merchant ed. U.S. Department of Health and Human Services, Public Health Service, Centers for Disease Control, National Institute for Occupational Safety and Health, DHHS (NIOSH) Publication No. 86-102, 801pp (pp.243-286).

Glenn R. E., and Craft, B. F. (1986) Air sampling for particulates. in Occupational Respiratory Diseases, James A. Merchant, ed. DHHS (NIOSH) Publication No. 86-102.

Hume, A., and Rimstidt J.D. (1992) The biodurability of chrysotile asbestos, American Mineralogist, v. 77, pp 1125-1128.

Kanapilly, G.M., Raabe, O.G., Goh, C.H.T., and Chimenti, R.A. (1973) Measurement of *in vitro* dissolution of aerosol particles for comparison to *in vivo* dissolution in the lower respiratory tract after inhalation. Health Physics, v. 24, pp. 497-507.

Lentner, Cornelius, Ed. (1984) Geigy Scientific Tables, Volume 3. (8th edition), 359 p. Medical Education Division, Ciba-Geigy Corporation, West Caldwell, NJ.

Lin, F., and Clemency, C.V. (1981) The dissolution kinetics of brucite, antigorite, talc, and phlogopite at room temperature and pressure. American Mineralogist, 66, 801-806.

Lehnert, B. (1992) Defense mechanisms and particle-cell interactions. in Health Effects of Mineral Dusts. George Guthrie and Brooke Mossman, Eds. Mineralogical Society of America. 427-469.

Luce, R.W., Bartlett, R.W. and Parks, G.A. (1972) Dissolution kinetics of magnesium silicates. Geochimica and Cosmochimica Acta, 36, pp 35-50.

Lund, L.G., and Aust, A.E. (1990) Iron mobilization from asbestos by chelators and ascorbic acid. Archives of Biochemistry and Biophysics, 278, 60-64.

McDonald, C. (1995) Silica, silicosis, and lung cancer: an epidemiological update. Applied Occupational and Environmental Hygiene, 10, 1056-1063.

Mossman, B.T. (1992) Cellular and molecular mechanisms of disease. in Health Effects of Mineral Dusts. George Guthrie and Brooke Mossman, Eds. Mineralogical Society of America. 513-521.

Nolan, R.P., and Langer, A.M. (1992) Limitations of the Stanton Hypothesis. in Health Effects of Mineral Dusts. George Guthrie and Brooke Mossman, Eds. Mineralogical Society of America. 309-326.

Rimstidt, J.D., and Newcomb, W (1993) Measurement and analysis of rate data: The rate of reaction of ferric iron with pyrite. Geochimica and Cosmochimica Acta, 57, 1919-1934.

Rimstidt, J.D. and Barnes, H.L. (1980) The kinetics of silica-water reactions. Geochimica and Cosmochimica Acta, 44, 1683-1699.

Robie, R.A., Hemmingway, B.S., and Fisher, J.R. (1979) Thermodynamic properties of minerals and related substances at 298.15 K and 1 bar pressure and at higher temperatures. U.S. Geological Survey Bulletin 1452. 456p.

Rosso, J.J. and Rimstidt J.D. (in prep) The statistical validity of rate constants: The olivine dissolution rate law.

Scholze, H., and Conradt, R. (1987), An *in vitro* study of the chemical durability of siliceous fibres. Annals of Occupational Hygiene, v. 31, no 4B, pp. 683-692.

Stanton, M.F., Layard, M. Tegeris, A., Miller, E., May, M., Morgan, E., and Smith, A. (1981) Relation of particle dimension to carcinogenicity of amphibole asbestsoses and other fibrous minerals. Journal of the National Cancer Institute, 67, 965-975.

Stayner, L.T., Dankovic, D.A., and Lemen, R.A. (1996) Occupational exposure to chrysotile asbestos and cancer risk: a review of the amphibole hypothesis. American Journal of Public Health, 86(2), pp 179-186.

Turpault, M.P. and Trotignon, L. (1994) The dissolution of biotite single crystals in dilute HNO_3 at 24 °C: Evidence of anisotropic corrosion process of micas in acidic solutions. Geochimica and Cosmochimica Acta, 58(13), pp. 2761-2775.

United States Department of Labor (1991) Occupational exposure to asbestos. 29 CFR 1910.1001. FR 59:40964-41162 August 10, 1994.

Werner, A.J., Hochella, M.F., Guthrie, G.D., Hardy, J.A., Aust, A.E., Rimstidt, J.D., (1995) Asbestiform riebeckite (crocidolite) dissolution in the presence of Fe chelators: Implications for mineral induced disease. American Mineralogist, 80, 1093-1103.

CHAPTER 3: BIOAVAILABILITY OF ARSENIC AND CHROMIUM FROM COAL FLY ASH

ABSTRACT

The bioavailability of As and Cr in a fine (1-10 μm) and a coarse (10-100 μm) particle split of coal fly ash from a power plant in the eastern U.S. was determined from time release profiles of these elements into physiologically-based solvents. Reaction of the fine split in Gamble's solution mimics the behavior of the fly ash in the pulmonary system and reaction of the coarse split in pH 2 HCl simulates the release of As and Cr to the gut. The time release data were incorporated into a toxicokinetic model to predict the biological response to As and Cr from occupational exposures to the coal fly ash. When occupational As and Cr exposures from coal fly ash were compared with referenced environmental exposure data, the predicted occupational exposure contributions from the ash relative to environmental exposures were found to be insignificant. The predicted biological exposure based on the geochemical investigation was compared with biological monitoring data from a cohort occupationally exposed to high arsenic coal fly ash and was found to estimate biological exposure within an order of magnitude. This favorable comparison supports the application of geochemical techniques to evaluate exposures to complex respirable materials.

INTRODUCTION

Coal is used world wide as a source of power and a large volume of coal ash is produced as a result. In 1996, approximately 730 million short tons of coal were burned in the United States, to generate 100 million short tons of coal ash (USDOE, 1997; ACAA, 1998). Improvements in stack control technology have resulted in significant reduction in total airborne particle emissions from coal plants. Nevertheless, the federal government has imposed regulations to limit particle emissions, reportedly in an effort to protect citizens from harmful exposures. These include recent regulations promulgated by the United States Environmental Protection Agency (USEPA) under the Clean Air Act limiting emissions of fine particulate matter, known as "PM 2.5". The USEPA defines particulate matter as "the generic term for a broad class of chemically and physically diverse substances that exist as discrete particles (liquid droplets or solids) over a wide range of sizes", and further defines PM 2.5 as "particles with an aerodynamic diameter less than or equal to a nominal 2.5 micrometers" (USEPA, 1997). Most ash is collected at the plant and landfilled, but some coal ash is utilized in a wide range of applications and products including flowable fill, road base, snow control, blasting, the manufacturing of roofing and wall board and in agriculture.

Most studies evaluating the effects of coal ash in the environment have focused on the behavior of disposed ash. These studies have investigated leachability of metals under disposal conditions (Wadge and Hutton, 1987; Grisafe et al., 1988; Jones, 1995). Environmental investigations have also evaluated the effects of exposure from coal fly ash to target species, with the goal of characterizing the effects of disposal on organisms in the environment (Suloway et al., 1983). Risk assessments evaluating broad effects of exposure on a wide geographic basis have been performed to document effects of stack emissions on the general population (EPRI,1994). However, relatively few studies have investigated the behavior of metals from complex materials such as coal ash in the body. Most work describing the toxicokinetics of arsenic have addressed fumes associated with metals smelting and other arsenic containing compounds (Vahter et al., 1986; Buchet et al., 1981). Yager et al. (1997) discussed urinary

arsenic excretion associated with occupational exposure to ash from a high arsenic coal. A geochemical measurement of metal's bioaccessibility has been performed; a batch reactor method was used to evaluate bioaccessibility of metals from soils in simulated gastric fluids (Hamel et al., 1998).

There are few reports of the effects of arsenic exposure from coal fly ash. Most studies have focused on As (III) exposures associated with copper smelting and arsenic trioxide production (Pinto et al., 1976; Smith et al., 1979; Vahter et al., 1986). It has been argued that the biological behavior of arsenic from these exposures is different than from coal fly ash (Yager et al., 1997). A study correlating arsenic exposure from coal fly ash and urinary arsenic output was performed on a cohort of workers from Slovakia. This group of workers was exposed to fly ash from a high arsenic coal. Arsenic exposure varied by worker class, and the authors correlated arsenic exposure to urinary arsenic elimination.

Industrial hygienists employ a range of techniques to evaluate occupational exposures to hazardous materials and other physical and chemical agents. These include measurement of the concentrations of agents in the breathing zones of workers and analysis of substances or their metabolites in biological specimens (typically urine and blood) to provide an estimate of actual exposure to workplace agents. These methods can be used to evaluate the total (occupational and non-occupational) exposure to a material. However, using biological samples evaluate the exposure after it has occurred so that any harm has already occurred by the time biological exposure data are available.

The ability to predict biological behavior of potentially toxic materials in a complex mixture before exposures occur would be extremely beneficial in order to prevent harm. However, evaluation of this behavior depends on several factors. For instance, the biological behavior of arsenic in coal ash is different from that of arsenic trioxide (Yager et al., 1997). Effects from inhalation exposure to a metal in a complex respirable material depend on the size distribution of the particulate matter and the chemical form of the element. Particle size controls the distribution of the particles between the pulmonary and

gastric systems. The deposition site then defines the chemical environment surrounding the particle and this and the chemical form of the element (e.g. oxidation state and compound) determines the release rate of the metal from the particle.

This paper describes the use of a mixed flow reactor method to measure the release rate of arsenic and chromium from two size splits of coal fly ash. Other reactor designs have been used to measure reaction rates, including batch reactors and plug flow reactors. A discussion of the use of various reactor designs to measure reaction rates is found in Rimstidt and Newcomb (1993). The purpose of this investigation is to estimate and evaluate the potential exposure to arsenic and chromium associated with inhalation of the ash in an occupational setting by defining their time release profile from respirable size particles. The time release profiles are integrated with a toxicokinetic model to predict behavior in the body. Comparison with the biological response of an occupationally exposed cohort was performed to test the predictive capability of the geochemical approach to estimate the degree and potential effects of exposure.

METHODS

Characterization of the ash sample

A sample of fly ash was obtained from a coal-fired power plant operated by an electric utility located in the eastern U.S. The sub-100 μm fraction was recovered using a mechanical tap and 100 μm mesh screen. The sub-100 μm fraction was further divided into two size splits using an Alpine Turboflex Model 50 ATP laboratory air classifier. A fine (sub-10 μm) split was recovered with the classifier operated with air flow of 10-15 mBAR (approximately 8,000 to 9,800 fpm). The classifier wheel was set at 22,000 rpm for recovery of the fine split. Approximately 38 percent (by weight) of the sub-100 μm fraction comprised this <10 μm split, as determined by size distribution analysis using a Cilas Granulometer 920. The coarse (10-100 μm) split comprised 62 weight percent of the sub 100 μm fraction. The waste from recovery of the fine split was used as feed stock for the recovery of the coarse

split. The classifier was operated with an airflow of 10-15 mBAR and a classifier speed of 4,000 rpm for this operation. Particle size distributions for the sub 100 μm feed material and the two recovered size splits were measured using a Cilas Granulometer 920. Cumulative size distribution curves for the three splits are shown in Figure 1.

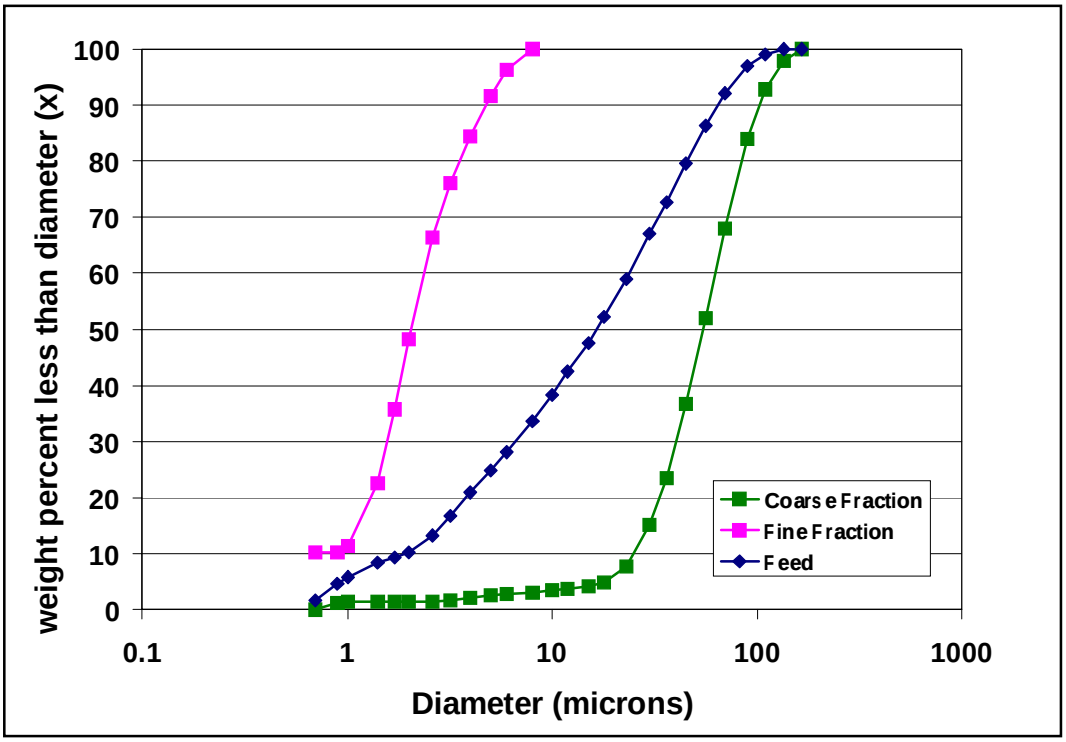

FIGURE 1. The curves shown the size distributions of the size splits used in this study. The "Feed" split was passed through a 100 μm screen. The fine split and coarse split were recovered from the feed material using a laboratory air classifier, and were used in the experiments defining time release profiles.

Transmission electron microscopy was used to characterize the morphology and elemental composition of particles in each size split. Samples of both coarse and fine ash splits were prepared for transmission electron microscopy following Asbestos Hazard Emergency Response Act (AHERA) methods (USEPA, 40 CFR Part 763 Appendix A to Subpart E). Qualitative observations were made on each of the size splits to determine particle morphologies and to identify particle compositions through energy dispersive X-ray analysis. Most of the particles in both were round aluminosilicate (spheres) containing small amounts of iron. These spheres comprised 90-95% of the particulate matter, by number. Spheres

observed in the fine split of the ash were usually in the range of 0.75 to 2.0 μm in diameter. Electron diffraction patterns were not readily observable due to the thickness of the particles. In addition, irregular agglomerations of fine particles up to 4-5 μm across were observed; these were composed of finer particles with diameters of approximately 0.03 μm. Energy Dispersive X-ray Analysis (EDXA) of these agglomerations indicated that iron is a major constituent, and that the agglomerations contain minor amounts of manganese, phosphorous, silicon, aluminum and calcium. Trace quantities of chromium, titanium, potassium and arsenic were noted in these fine particles. The accumulation of these metals as discreet particles is contrary to commonly reported observations that trace metals occur as coatings on particle surfaces (Smith et al., 1979). These fine particles may represent a condensing aerosol phase of the combustion process, may be present in substituted minerals such as spinel, or a combination of these mechanisms (Pacyna, 1986; Hulett et al., 1980).

A sample of each split was analyzed on a Sintag X-ray Diffractometer using Cu Kα radiation. Background subtractions were performed, and residual spectra for the coarse and fine splits are shown in Appendix B. Mullite and quartz were identified in the powder diffraction patterns of the ash samples with the relative proportions of mullite (compared with quartz) being greater in the fine split of the ash. Trace quantities of hematite (?) were observed in the XRD pattern of the coarse ash split.

Surface areas of the two size splits were measured using a Quantichrome Surface Area Analyzer following the method of Brunauer, et al. (1938) using nitrogen as the adsorbate gas. The samples were degassed at 125° C under a vacuum for approximately 2 hours prior to analysis. The fine split had a specific surface area of 5.3 m^2/gm. The coarse split had a specific surface area of 2.3 m^2/gm.

Qualitative verification of the sulfate content of the ash splits was performed. Ten grams of each size split of coal ash were suspended in a beaker with 100 mL of deionized water using a magnetic stirrer.

The pH of the suspension dropped 1.4 units immediately after addition of the fine split of fly ash. The sample was agitated for 30 minutes, then allowed to settle. The supernatant was decanted and mixed with a solution of 0.5M $Ba(NO_3)_2$. A white precipitate formed upon mixing. Similar qualitative findings were observed in the coarse ash fraction, although the pH of the coarse ash suspension increased approximately 4.5 pH units with addition of the coarse ash to the deionized water. Suspensions of the fine ash split were acidic while suspensions of the coarse split were alkaline.

Nitric acid extractions were performed on samples of the fine and coarse splits of ash. Both size splits of 1) unreacted ash, 2) ash reacted in the Gamble's solution and 3) pH 2 HCl solvent were analyzed. Known weights (approximately 250 to 320 mg) of sample were extracted using 5 mL of 70% HNO_3. Samples were placed on a hot plate at 70 °C for 5 hours. The acid extract was diluted to 25 mL, filtered, and then aspirated directly into the Inductively Coupled Plasma (ICP) instrument for analysis. The bulk sample metal data are included in Table 1.

TABLE 1. As and Cr concentrations of the coal ash used in our experiments based on digestion in concentrated nitric acid. The Gamble's solution reacted fly ash and pH 2 HCl reacted fly ash samples were recovered from the reactor after completion of the experiments.

	Chromium (ppm)		Arsenic (ppm)	
	<10 μm	10-100 μm	<10 μm	10-100 μm
Unreacted Fly Ash	75	20	76	<DL
Gamble's Reacted Fly Ash	66	12	33	<DL
pH 2 HCl Reacted Fly Ash	60	13	74	<DL

Solution preparation, reaction and analysis

Two series of experiments were performed on each size split of ash. Release rates of arsenic and chromium were determined for each size split in modified Gamble's solution and in a pH 2 hydrochloric acid solution. The modified Gamble's solution was prepared following the derivation of Scholze and Conradt (1987). Ova albumen was added to the solution in concentrations consistent with the proteins in the intercelluar fluid (Gamble, 1942). Albumen was chosen as the protein surrogate since it is the most

abundant protein in serum plasma (Lentner, 1984). The composition of the Gamble's solutions used in our experiments is included in Table 2.

TABLE 2. Concentration of the components of the modified Gamble's solution used in our experiments.

Component	Concentration (mg/L)
$MgCl_2 \bullet 6H_2O$	212
NaCl	6,400
$CaCl_2 \bullet 2H_2O$	255
$Na_2SO_4 \bullet 10H_2O$	179
Na_2HPO_4	148
$NaHCO_3$	2,700
Na_2 tartrate$\bullet 2H_2O$	180
Na_3 citrate$\bullet 2H_2O$	153
Na lactate (60% w/w)	290
Glycine	118
Na pyruvate	172
ova albumen	445

Measurements of release rates were performed using a mixed flow reactor modified from the design described by Rimstidt and Newcomb (1993). A 125 mL reaction vessel constructed of acrylic plastic was used. Figure 2 shows a schematic diagram of the experimental system. The solids were suspended in solution using a wrist-action shaker and each experiment was performed three times. For each experiment, 10 grams of ash were loaded into the reactor. Solvent solutions were pumped through the system using a peristaltic pump at flow rates that averaged approximately 0.2 g/min for the Gamble's solution, and 0.8 g/min for the pH 2 solution. The flow rate was determined by timing the collection of effluent into pre-weighed 30 mL polyethylene bottles. The pH of the effluent was monitored with an in-line Beckman phi 72 pH meter equipped with an Accumet electrode. pH data were collected at defined times (typically every 15 minutes) using a serial printer interfaced to the pH meter. Samples of the effluent were collected in series during the first four hours of the experiment and were collected periodically thereafter throughout the duration of the experiment. The time to collect 30 mL of reactor effluent varied with the flow rate of the reactor system. Experiments using Gamble's solution had lower flow rates compared with the pH 2 HCl determinations likely resulting from the higher viscosity of the

protein in the Gamble's solution. Experiments were performed for periods of up to three days. Effluent was collected into acid washed, triply (deionized water) rinsed 30 mL polyethylene bottles. The pH of the effluent and the flow rate were recorded at the time of sample collection. All samples were acidified with 1 mL of concentrated nitric acid, then stored refrigerated prior to analysis.

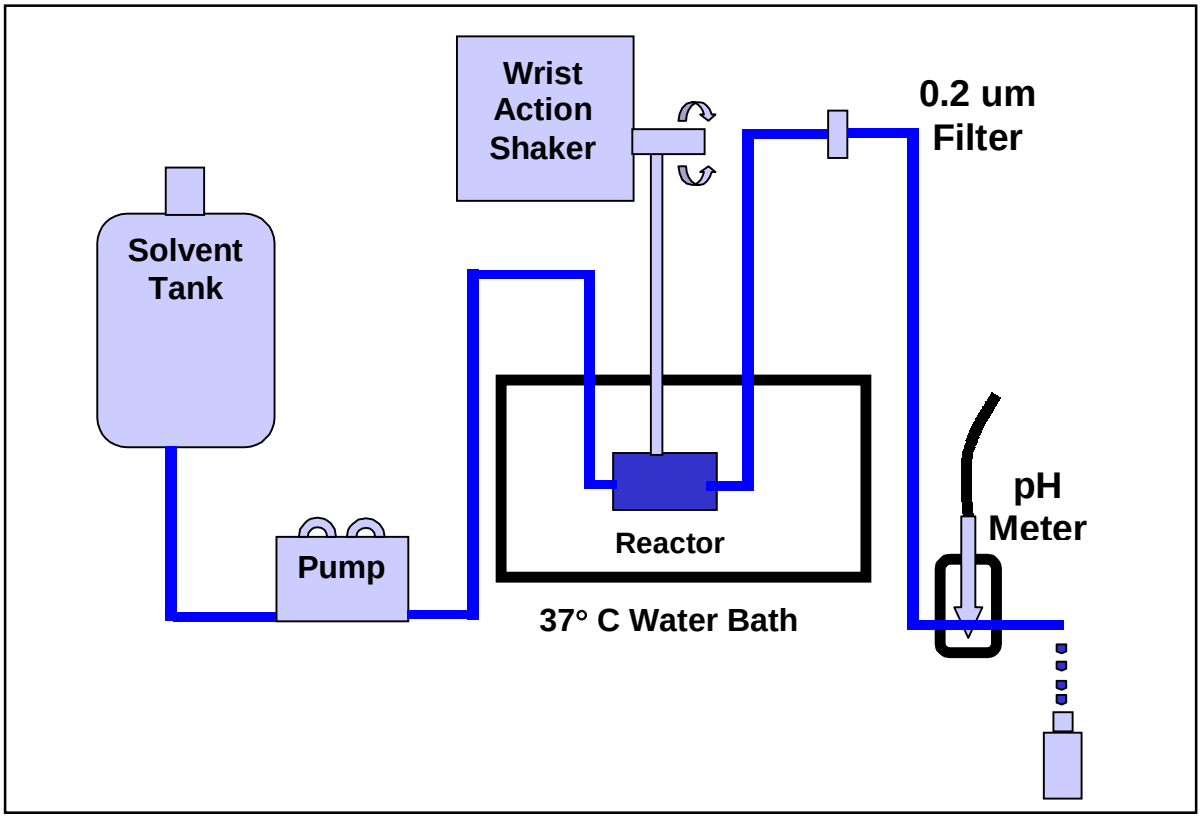

FIGURE 2. The drawing shows the components of the mixed flow reactor system. Solvent is pumped into the reactor vessel containing the coal ash, which is constantly agitated using a wrist-action shaker. The temperature is maintained at 37°C by immersion in a constant temperature water bath. The effluent pH is monitored by an in-line electrode mounted in a flow through cell. Samples of effluent are collected from the flow through cell.

The As, Cd, Cr, and Pb contents of the samples were determined using ICP analyses. Concentrations were proportional to the integrated intensity of the As 193.7 nm peak, Cr 283.5 nm peak, Cd 228.8 nm peak and the Pb 220.3 nm peak. Concentrations were referenced to standard solutions prepared from 1000 ppm analytical standards. Detection limits were 22 ppb for As, 3.2 ppb for Cr, 3.2 ppb for Cd, and 35 ppb for lead. Replicate analyses indicated a relative percent standard deviation of 6.6% for As, 5.9% for Cd, 5.2% for Cr, and 7.9% for Pb. The protein-free samples were analyzed directly without dilution.

Protein was coagulated and precipitated from albumen-containing samples by the addition of nitric acid. The protein was separated from the solution by centrifugation at 5,000 g followed by filtration of the supernatant. The recovered supernatant was aspirated directly into the ICP for analysis. Analysis of the solvent blanks did not detect the presence of As, Cd, Cr, or Pb above the analytical limit of detection.

ANALYTICAL RESULTS

The metal release rates were calculated from measured effluent concentrations of arsenic and chromium from both size splits of ash in pH 2 HCl and Gamble's solution (Table 3). Only the measured arsenic and chromium concentrations and the pH of the effluent solution are tabulated; the lead concentrations were all below detection and although small concentrations of cadmium were detected in samples collected at the beginnings of some experiments, they were not significant enough to include in an occupational exposure model. All data from these experiments are available in Appendix B.

TABLE 3. Results of the mixed flow reactor experiments. The table includes the weigh of each sample collected, the start and stop time of sample collection relative to the beginning of the experiment, and the As and Cr concentrations of each sample. The heading for each group of data indicate the type of experiment. FG = fine split in Gamble's solution, FA = fine split in pH 2 HCl, CG = coarse split in Gamble's solution, CA = coarse split in pH 2 HCl, <DL = less than detection limit. The number following the initials indicates the replicate run number. Individual numbers listed in the vertical # column indicate the order by which the samples were collected during the experiment.

#	Weight of Collection (g)	Start Time (min)	Finish Time (min)	As (ppm)	Cr (ppm)
FG1					
1	28.6	1	38	0.13	0.083
2	29.6	40	90	1.2	0.16
3	30.2	91	143	2.6	0.11
4	28.7	144	195	2.0	0.067
5	34.4	196	266	1.4	0.053
6	29.2	266	329	1.1	0.047
7	29.4	330	398	0.86	0.043
8	31.2	665	765	0.58	0.035
9	33.1	1461	1616	0.29	0.029
10	30.3	2001	2190	0.22	0.027
11	35.2	2640	2995	0.22	0.027

#	Weight of Collection (g)	Start Time (min)	Finish Time (min)	As (ppm)	Cr (ppm)
FG2					
1	30.5	1	52	0.19	0.087
2	32.6	53	123	1.7	0.15
3	31.3	124	212	2.7	0.12
4	36.5	213	327	1.8	0.079
5	33.6	328	448	1.2	0.062
6	35.7	450	584	0.88	0.052
7	32.8	585	719	0.77	0.048
8	31.2	1286	1455	0.28	0.035
9	27.9	1908	2088	0.20	0.031
10	32.5	2456	2700	0.16	0.029
FG3					
1	31.3	2	111	0.15	0.041
2	36.4	113	279	1.6	0.13
3	28.0	280	419	1.8	0.084
4	34.2	420	603	1.2	0.061
5	31.6	604	784	0.80	0.047
6	36.9	1047	1307	0.32	0.033
7	29.0	1869	2119	0.22	0.024
8	30.5	2489	2809	0.20	0.035
9	31.4	3189	3541	0.19	0.035
10	30.6	3848	4211	0.079	0.014
11	33.1	4736	5156	0.078	0.0095
12	30.7	6133	6559	0.070	0.0077
13	33.7	7025	7500	0.081	0.0062
FA1					
1	25.8	0	37	< DL	0.93
2	23.2	37	75	< DL	0.27
3	18.9	76	113	< DL	0.23
4	22.5	113	152	< DL	0.28
5	30.3	152	192	< DL	0.16
6	34.4	192	232	< DL	0.12
7	25.0	232	272	< DL	0.094
8	30.2	272	312	< DL	0.082
9	26.6	312	352	< DL	0.074
10	30.9	352	392	< DL	0.070
11	22.0	704	744	< DL	<DL
FA2					
1	22.5	1	45	< DL	1.3
2	22.4	45	88	< DL	0.41
3	20.6	88	131	< DL	0.22
4	22.1	132	175	< DL	0.17
5	18.7	175	218	< DL	0.13
6	20.7	218	261	< DL	0.098

#	Weight of Collection (g)	Start Time (min)	Finish Time (min)	As (ppm)	Cr (ppm)
7	24.8	261	301	< DL	0.073
8	21.2	301	341	< DL	0.060
9	15.9	341	388	< DL	0.050
10	18.5	389	431	< DL	0.050
11	25.3	711	751	< DL	0.032
FA3					
1	29.0	3	53	< DL	1.3
2	33.4	53	103	< DL	0.34
3	34.8	103	153	< DL	0.21
4	32.2	153	198	< DL	0.18
5	37.2	198	248	< DL	0.14
6	33.3	248	293	< DL	0.11
7	33.3	293	338	< DL	0.084
8	34.4	339	384	< DL	0.072
9	33.9	384	429	< DL	0.062
10	34.3	429	474	< DL	0.054
11	36.5	926	976	< DL	0.031
12	37.5	1310	1360	< DL	0.019
13	33.7	1789	1834	< DL	0.0097
14	36.4	2297	2347	< DL	0.0024
CG1					
1	29.6	0	130	0.48	0.086
2	24.6	135	277	0.34	0.039
3	25.5	706	1097	0.14	0.028
4	30.5	1099	1672	0.13	0.028
5	25.6	1672	2235	0.11	0.028
6	29.1	2236	2968	0.072	0.027
7	37.9	2971	4184	<DL	0.024
8	28.9	4184	5147	<DL	0.024
CG2					
1	29.4	1	128	0.49	0.070
2	28.5	130	276	0.29	0.042
3	36.3	278	511	0.12	0.034
4	29.7	511	769	<DL	0.030
5	32.8	770	1115	<DL	0.029
6	37.6	1115	1594	<DL	0.028
7	29.9	1594	2023	<DL	0.024
8	37.6	2025	2644	<DL	0.022
9	19.4	2649	3344	<DL	0.021
CG3					
1	31.4	2	26	0.096	0.038
2	38.2	27	90	0.024	0.018
3	25.9	93	136	0.074	0.016
4	37.8	137	289	<DL	0.015

#	Weight of Collection (g)	Start Time (min)	Finish Time (min)	As (ppm)	Cr (ppm)
5	27.2	289	346	<DL	0.015
6	32.0	349	447	<DL	0.018
7	39.1	448	576	<DL	0.025
8	28.9	992	1084	<DL	0.021
9	36.4	1789	1905	<DL	0.017
10	31.9	2440	2539	<DL	0.014
CA1					
1	30.3	0	42	0.42	0.24
2	34.4	43	90	0.31	0.16
3	32.5	90	135	0.16	0.090
4	34.2	135	188	0.16	0.066
5	28.7	188	227	0.087	0.051
6	30.7	227	271	0.12	0.042
7	28.9	272	311	0.080	0.034
8	33.1	539	584	0.058	0.020
9	30.2	996	1085	0.041	0.013
CA2					
1	29.7	1	43	0.15	0.13
2	29.9	44	86	0.25	0.11
3	30.0	86	128	0.17	0.075
4	31.0	128	170	0.10	0.050
5	33.0	170	212	0.065	0.035
6	31.9	212	252	0.041	0.024
7	32.1	253	293	0.049	0.018
8	32.4	293	333	0.035	0.013
9	31.3	459	499	0.033	0.0078
10	29.1	885	924	<DL	0.0033
CA3					
1	32.6	1	41	0.18	0.14
2	31.9	41	81	0.28	0.096
3	31.8	81	121	0.19	0.054
4	31.8	121	161	0.11	0.032
5	32.0	161	201	0.047	0.022
6	33.9	201	244	0.063	0.013
7	31.8	244	284	0.067	0.0080
8	31.8	284	324	0.036	<DL
9	31.9	324	364	0.043	<DL
10	34.0	736	779	<DL	<DL

Representative experiments are shown in Figures 3 and 4, and include the reaction of the fine ash split in Gamble's solution (Figure 3) and reaction of the coarse ash split in pH 2 HCl (Figure 4). These two

series of experiments served as the basis for the occupational component of the arsenic and chromium dose in our toxicokinetic model. The figures plot effluent pH and the rates of arsenic and chromium release to solution against time from the start of the experiment. A normalized reaction rate , k (moles /m^2 sec), was calculated for each sample using the experimental flow rate, effluent arsenic and chromium concentrations, the weight of ash in the reactor (10g) of Table 3 and the sample specific surface area using the following equation:

$$k(\frac{moleAs,Cr}{M^2 \bullet \sec}) = \frac{flowrate(\frac{kg}{\sec}) \bullet As,Cr(\frac{mole}{kg})}{SampleWeight(g) \bullet SpecificSurfaceArea(\frac{M^2}{g})}$$

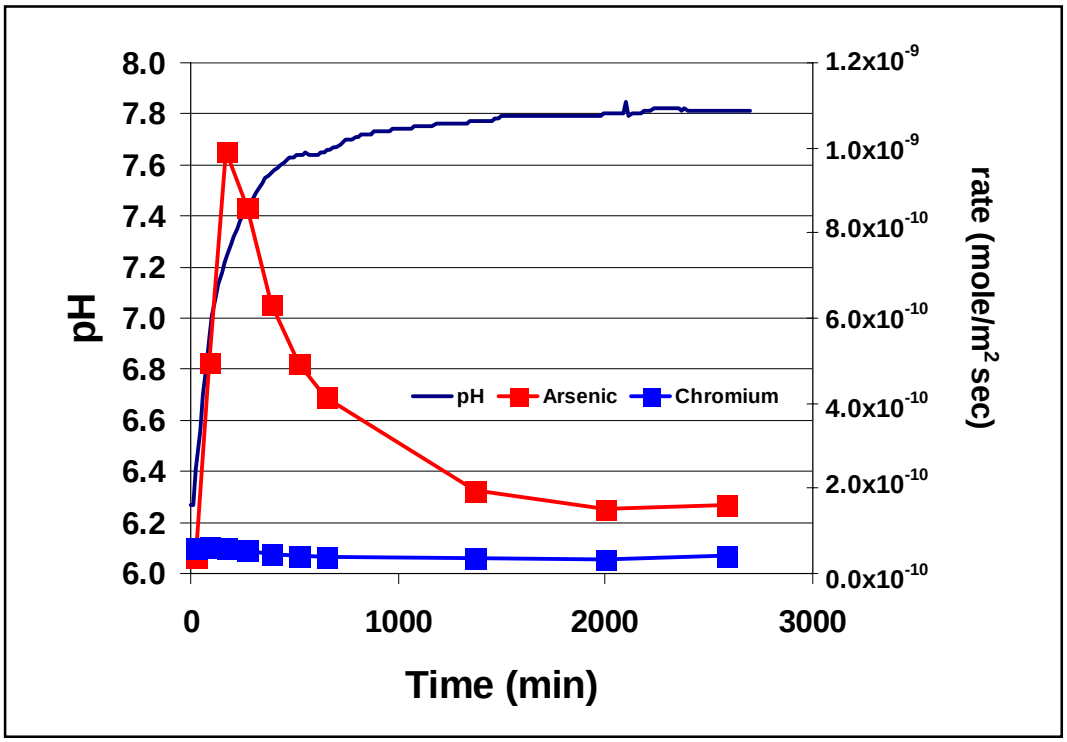

FIGURE 3. This plot shows a typical experimental run for the fine ash split in the Gamble's solution used to simulate arsenic and chromium release to the lung. Effluent pH is plotted on the left vertical axis, and the measured release rate of arsenic and chromium is plotted on the right vertical axis. The experiments were characterized by an initial small increase in pH, followed by a gradual decline to the pH of the solvent pumped into the reactor. Chromium release rates decreased through the experimental run. Measured arsenic release rates typically increased during collection of the first two samples, then decreased through the remainder of the experiment.

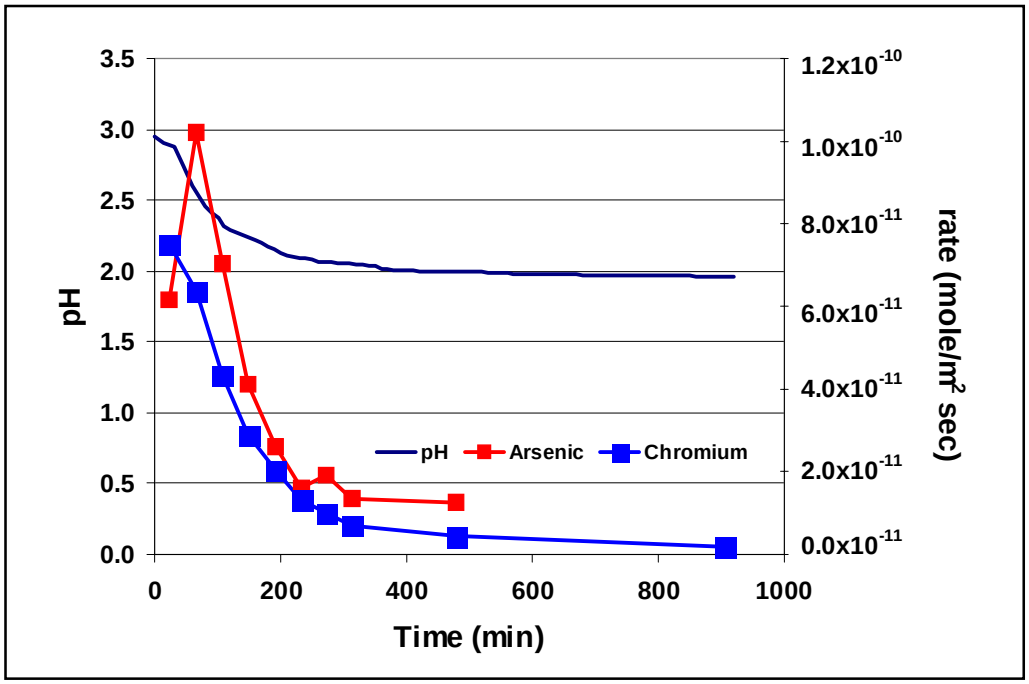

FIGURE 4. This plot shows a typical experimental run for the coarse ash split in the pH 2 HCl used to simulate arsenic and chromium release to the gut. Effluent pH is plotted on the left vertical axis, and the measured release rate of arsenic and chromium is plotted on the right vertical axis. The experiments were characterized by an initial small increase in pH, followed by a gradual decline to the pH of the solvent pumped into the reactor. Chromium release rates decreased through the experimental run. Measured arsenic release rates typically increased during collection of the first two samples, then decreased through the remainder of the experiment.

The calculated rate was plotted at the mid-point (in time) of the period of sample collection. Initial reactions between the Gamble's solution and the fine coal ash split resulted in a decrease of pH from approximately 7.8 to 6.3. This decrease was attributed to an immediate release of sulfuric acid from the fine ash split at the beginning of the experiment. The coarse ash split was alkaline, and initial reactions between the coarse fraction of the coal ash and the pH 2 HCl solvent resulted in a pH increase of approximately 1 pH unit. The initial rate of arsenic release to solution in our experiments may represent a transient non-steady state condition due to an initial slow release of arsenic from the coal ash to the solution flowing through the reactor. If such mechanically induced delays related to the initial filling of the reactor occurred, the net effect would be to alter the shape of the time release profile. The estimate of

the amount of bioavailable arsenic released from the ash over the course of the experiment would not be affected. The rate of arsenic release peaks approximately 1 hour after the start of the experiment, then decreases through the duration of the experiment. This observed rate decrease may result from the mixing properties of the reactor, or may be the result of the dissolution of arsenic initially present on the surface of the particles followed by the diffusion-limited release of arsenic contained within the ash particles.

DISCUSSION

Industrial Hygiene

Industrial hygiene methods that estimate actual exposure are based on measuring the concentration of an agent or its metabolite in body fluids such as urine or blood. These are known as biological exposure indices (BEI's) (ACGIH, 1997). A major drawback of the BEI's is that the approach measures exposures and indicates overexposures only after they occur. The interpretation of data from biological specimens is further limited by uncertainties introduced by a wide range of physiological parameters such as differences in body size, conditioning of the worker, previous exposures, and environmental differences (ACGIH, 1993). For example, the volume of daily urine output can vary by a factor of four, while the weight of solids excreted in the urine may vary by a factor of two (Lentner, 1981; Wallach, 1986). Urinary concentrations of arsenic and similar metals are not useful measures of exposure by themselves. Urinary production rates vary considerably in an individual through the day and urinary production rates also vary between individuals. For these reasons, arsenic concentrations in urine are normalized to the creatinine content of the urine. Creatinine is produced by the metabolism of proteins and is eliminated from the body through urine at a relatively constant rate. It is therefore an internal standard for determining the "metabolic" volume of urine being produced. Referenced values of daily creatinine elimination range from 1.46 g/day for a study of 138 adults (Szadkowski et al., 1970) to 1.8 g/day for 19 adult males (Vestergaard and Leverett, 1958).

Industrial hygienists routinely evaluate workplace concentrations of materials such as arsenic and chromium , which are both human carcinogens under certain conditions, to assess and control hazards associated with exposures to these substances. Measured concentrations of agents in the worker's "breathing zone" are typically compared with published occupational exposure control limits to evaluate the potential for overexposure. Methods used to perform these evaluations have been developed by the National Institute for Occupational Safety and Health (NIOSH) and OSHA and typically have uncertainties on the order of ± 25% when field and laboratory errors are considered. The American Conference of Governmental Industrial Hygienists (ACGIH) recommends Threshold Limit Values (TLVs) to limit occupational exposures to workplace stressors. These TLVs are reviewed and published annually and are considered "state of the art" exposure guidelines. For most chemical agents, including nuisance dusts, aresenic, and chromium, conformance with the TLV is determined via 8-hour time weighted averages (TWAs), which are measured with samples collected over extended periods of time, usually ranging from four to eight hours. These TWA samples represent the average concentration over the sampling period, and do not indicate peak exposures; these samples further represent conditions under which it is believed that workers may be repeatedly exposed, day after day, without adverse effect.

Occupational exposure limits are listed for many well characterized materials but risks associated with complex mixtures, such as coal fly ash, are difficult to evaluate. The presence of a complex mixture of metals which target similar organs or other biochemical systems presents the potential for synergistic deleterious effects. It is therefore critical to evaluate accurately the amounts of materials actually available for uptake into the body. Inaccurate assessment of the bioavailability of an agent from a complex mixture may lead to an overestimation of actual dose. Failure to identify a synergistic exposure or a biologically active component may result in an underestimation of the hazards related to exposure. When evaluating materials to assess the potential for hazardous exposures, screening evaluations such as the one developed here offer a valuable way to predict behavior of an agent in the body.

Occupational arsenic exposures occur in several industries, including the manufacture of semiconductors, and in the manufacture and use of certain pesticides, herbicides, and insecticides, including wood preservative treatments with arsenic salts. Arsenic in coal fly ash occurs almost exclusively as As (V) (Wadge and Hutton, 1987). Chronic exposures to arsenic affect several systems within the body, including the skin, upper respiratory system, central nervous system, and the gastrointestinal tract (Amdur et al., 1991). Arsenic is considered a known human carcinogen, and is associated with cancers of the skin and liver (ACGIH, 1993). Arsenic occurs naturally in several valence states, including As (III) and As (V). Redox reactions involving arsenic occur in the body, and As (V) is reduced to As (III). Reduction to As (III) is likely a precusor to methlylation, based on in vitro studies (Buchet and Lauwerys 1985, 1988, Lerman et al., 1983). Methylation of inorganic arsenic (A_i) to dimethyarsinic acid (DMA) and monomethyarsonic acid (MMA) occurs in the liver as part of the body's detoxification process. Urinary MMA, DMA and A_i concentrations have been used as biological indicators of arsenic exposure (Bouchet et al., 1981, Vahter et al., 1986). Approximately 60% of absorbed arsenic is eliminated through the urine (Buchet et al., 1981). Arsenic is also excreted through the skin, sweat, nails, feces, and hair. The 1997 ACGIH TLV for inorganic arsenic is 0.01 mg/m^3 and the exposure limit does not vary based on oxidation state.

Occupational exposures to chromium occur in a wide range of industries. Significant exposures may occur in mining and processing chromite ore, in metal plating operations and while welding stainless steel. Chromium occurs in three valence states in the work place as chromium metal (0), and as chromic (III) and chromate (VI) salts. Exposures to chromium have been related to perforation of the nasal septum and allergic skin reactions (Amdur et al., 1991) Of all the oxidation states, chromium (VI) presents the greatest exposure risk because it is associated with upper respiratory cancers. Chromium is a micronutrient in the diet, and is essential for the metabolism of glucose, protein and fat (ATSDR, 1991b). Water soluble chromium (VI) compounds are predominantly removed through the urine, although some

chromium is eliminated from the body through hair, nails and feces (ATSDR, 1991b). The 1997 ACGIH TLV for chromium (VI) compounds is 0.01 mg/m^3. Exposure limits for chromium (III) compounds are higher.

Both chromium and arsenic are present in the environment, and both metals are stored to some extent in the body. Non-occupational exposures to both arsenic and chromium occur from the air and from consumption of food and water. Uptake of arsenic from the environment was estimated as 0.2 μg/day from air, 0.04 mg/day from food, and 0.015 mg/day from water (ACGIH, 1996; ATSDR, 1991a; WHO, 1983). Uptake of chromium was estimated as 0.4 μg/day from air, 60 μg/day from food, and 0.2 μg/day from water (ATSDR, 1991b, Bennet, 1986).

General dust exposures occur in a range of occupational settings. Many such exposures are associated with "nuisance" dusts that do not contain specifically hazardous materials. Nuisance dusts, as defined by ACGIH, do not contain asbestos, and contain < 1% crystalline silica. Occupational exposure limits for dusts protect against excessive insult to the respiratory system from airborne particulate matter. Occupational exposure control limits for dusts are different for "inhalable", and "respirable" fractions, which limits are based, in part, on the sensitivity of the deep lung to damage from inhaled particles. The size of a particle generally controls the deposition site in the pulmonary system and the site of deposition defines the chemical environment surrounding the deposited particulate matter. Several defense mechanisms protect the lung against damage from inhaled dusts. Scavenger cells (macrophages and leucocytes) are activated in response to dust deposition and these cells engulf and remove particulate matter from airway surfaces. The upper reaches of the respiratory tract are protected by the "mucociliary escalator", which consists of a blanket of mucous that is constantly moved upward by the beating of cilia. Particles removed via the mucociliary escalator are either expectorated or ingested, leading to an oral exposure through the chemically harsh environment of the digestive system. Larger particles deposited

on the upper reaches of the respiratory system may be translocated within a few hours past exposure (Lehnert, 1992, Morrow, et al., 1967). The amount of inhaled dust taken up during a work shift is the product of several factors. The time weighted average dust concentration, exposure duration, and the amount of air inhaled during the exposure period define the amount of dust entering the respiratory system. Respiratory volumes depend on the conditioning of the worker, and the level of activity. The ACGIH recommends controlling exposures to 3 mg/m^3 for the respirable fraction, and 10 mg/m^3 for the inhalable fraction (ACGIH, 1997). Size selective sampling techniques employing nylon cyclones or other methods are commonly used to measure respirable dusts.

Conceptual Model

Toxicokinetic models are used to evaluate the movement of materials through the body. Several general types of toxicokinetic models are used, based on the approach used to describe the fate of agents within the body, including descriptive (mathematical) models and predictive (physiologically-based) models (ACGIH, 1993; Fisherova-Bergerova, 1990). In each case, compartments are defined, and the rate of elimination from the body is described as a function of the partitioning of an agent into the compartments and the rates of transfer of the agent or its metabolite between compartments. Predictive models incorporate physiologically-based compartments, such as the liver, kidneys, and circulatory system. Compartments in descriptive toxicokinetic models are mathematical entities that do not necessarily correspond with physiological systems, but are based on specific rates of decay observed in the elimination curves measured from exposed populations. Elimination curves typically show an exponential decay, and the elimination rate constants for descriptive toxicokinetic models are determined from the slopes of curves fit to the elimination data.

The purpose of this study was to investigate the feasibility of using a “benchtop” geochemical experiment to furnish input on bioavailability for an industrial hygiene dose-response model and to predict the results of exposure to arsenic and chromium in coal fly ash. The ability to predict the effects of an exposure

before it occurs is extremely beneficial, since this knowledge can be used to protect workers by avoiding conditions that result in overexposure. This report demonstrates a procedure which uses measured rates of arsenic and chromium release in a benchtop experiment to estimate occupational exposure uptake by combining our experimental results with a hypothetical occupational coal fly ash dust exposure to predict the resulting bioavailability of arsenic and chromium from the inhaled coal ash. The coal fly ash used for our experiments did not contain sufficient arsenic or chromium to consider application of the individual TLVs for the chromium or arsenic, so the hypothetical occupational coal fly ash exposure was treated as a dust exposure. The modeled behavior of arsenic was then compared with the observed behavior of arsenic in a cohort occupationally exposed to coal fly ash to evaluate the predictive capability of our model.

The model developed here simulates the body's response to doses of arsenic and chromium and predicts the fate over time of a series of consecutive daily doses from both occupational and environmental sources. The "occupational" doses are described by the timed release profiles for the fine and coarse ash splits. Two series of experiments were used to measure metals release into the body from the coal fly ash. Release of arsenic and chromium from the fine ash split into Gamble's solution was used to model metals release in the pulmonary environment. Release rates of arsenic and chromium from the coarse ash split into pH 2 HCl were used to estimate the timed release profile into the digestive system. The coarse ash data were used to represent metals release into the gut after translocation from the respiratory system via the mucociliary escalator. Arsenic and chromium contributions from air, food, and water were combined with these occupational doses derived from the inhalation exposure to the coal fly ash.

Experimental Results

The characterization of the coal fly ash used in our experiments indicated that the size splits were chemically distinct. The concentrations of arsenic and chromium were greater in the fine split than in the coarse split. The enrichment of arsenic and chromium in the finer sized particles is consistent with

findings from other studies of the concentration dependence on particle size in coal ash (Smith, 1979; Davison et al., 1974). These findings are also consistent with our observation of very fine iron-rich particles containing a wide range of trace elements, including both arsenic and chromium. Coal ash has been described as either alkaline or acidic, and these differences have been related to the chemical composition of the ash, with acidic behavior associated with low calcium ashes and alkaline behavior associated with high calcium ashes (Grisafe et al., 1988). In our sample, the pH of suspensions of the fine ash split was acidic and this effect was attributed to the presence of sulfuric acid present on the particle surface. The coarse ash split was alkaline. This variation in chemical behavior was observed in the experiments using the different ash fractions, and verified by suspension of the two fractions in distilled water and measuring the resulting pH over time. These size dependent variations in chemistry are likely an important factor in the behavior of coal ash particles deposited in the different environments within the body.

The experimental results were recast to normalize the effects of the variable flow rates and to define the time release profiles of arsenic and chromium from both size splits of ash into the Gamble's solution and the pH 2 HCl. The amount of arsenic and chromium released by 10 g of ash was calculated in hourly increments from the individual sample results. Release rates in terms of ng of metal per minute were determined for each sample assuming the metal release into solution was constant across each sample collection interval. Hourly intervals that were defined by multiple samples were calculated using weighted release rates per minute based on the corresponding percentage of time for each rate. The amounts of chromium and arsenic released from 10 grams of ash per hour, based on manual integration of the sample collection times and the calculated rates of release are summarized in Table 4 and are shown graphically in Figures 5 and 6.

TABLE 4. Normalized hourly arsenic and chromium release per 10 g Coal Fly Ash. These data were obtained by calculating a time weighted amount of arsenic and chromium released during the individual experiments. CA indicates results from experiments on the coarse split of ash in pH 2 HCl and CG results are from the experiments on the coarse ash split in Gamble's solution. Similarly, FA results are from the experiments on the fine ash split in pH2 HCl, and the FG results are from the experiments on the fine ash split in the Gamble's solution. The standard deviation (s) is included when there were more than one data point for a given hourly interval. The number (n) of experiments that contributed to the calculated hourly release is included. Blank entries indicate that no data were available for the hourly interval.

	Arsenic (μg)						Chromium (μg)					
Hour	**1st Run**	**2nd Run**	**3rd Run**	**avg.**	***s***	***n***	**1st Run**	**2nd Run**	**3rd Run**	**avg.**	***s***	***n***
CA												
1	16.8	7.54	10.2	11.5	4.8	3	9.31	5.14	6.03	6.8	2.2	3
2	10.3	8.8	10.6	9.9	1.0	3	5.39	3.8	3.2	4.1	1.1	3
3	6.28	4.62	4.35	5.1	1.0	3	2.9	2.18	1.35	2.1	0.8	3
4	4.37	2.49	2.75	3.2	1.0	3	2.22	1.46		1.8	0.5	2
5	4.29	2.2	2.72	3.1	1.1	3	1.66			1.7		1
6			2.28	2.3		1						
CG												
1	6.6	6.8	3.51	5.6	1.8	3	1.15	0.99		1.1	0.1	2
2	6.6	6.8	1.78	5.1	2.8	3	1.15	0.99		1.1	0.1	2
3	4.28	3.81		4.0	0.3	2	0.53	0.55		0.5	0.0	2
4	3.55	3.41		3.5	0.1	2	0.42	0.49		0.5	0.1	2
5		2.47		2.5		1		0.42		0.4		1
6		1.16		1.2		1		0.31		0.3		1
FA												
1							34.2	42.6	39.7	38.8	4.3	3
2							11.4	12.9	12.2	12.2	0.8	3
3							9.02	7.9	8.34	8.4	0.6	3
4							5.78	5.35	6.66	5.9	0.7	3
5							4.21	3.98	4.82	4.3	0.4	3
6							3.51	2.44	3.58	3.2	0.6	3
FG												
1	16.1	12.8	2.58	10.5	7.0	3	4.24	3.2	0.72	2.7	1.8	3
2	66.3	47.2	5.79	39.8	30.9	3	4.66	4.28	0.87	3.3	2.1	3
3	73.9	57	21.8	50.9	26.6	3	2.84	2.52	1.66	2.3	0.6	3
4	46.4	46.4	21.8	38.2	14.2	3	1.7	2	1.66	1.8	0.2	3
5	34.5	34.6	21.9	30.3	7.3	3	1.42	1.53	1.43	1.5	0.1	3
6	26.1	27	22	25.0	2.7	3	1.23	1.26	1.04	1.2	0.1	3

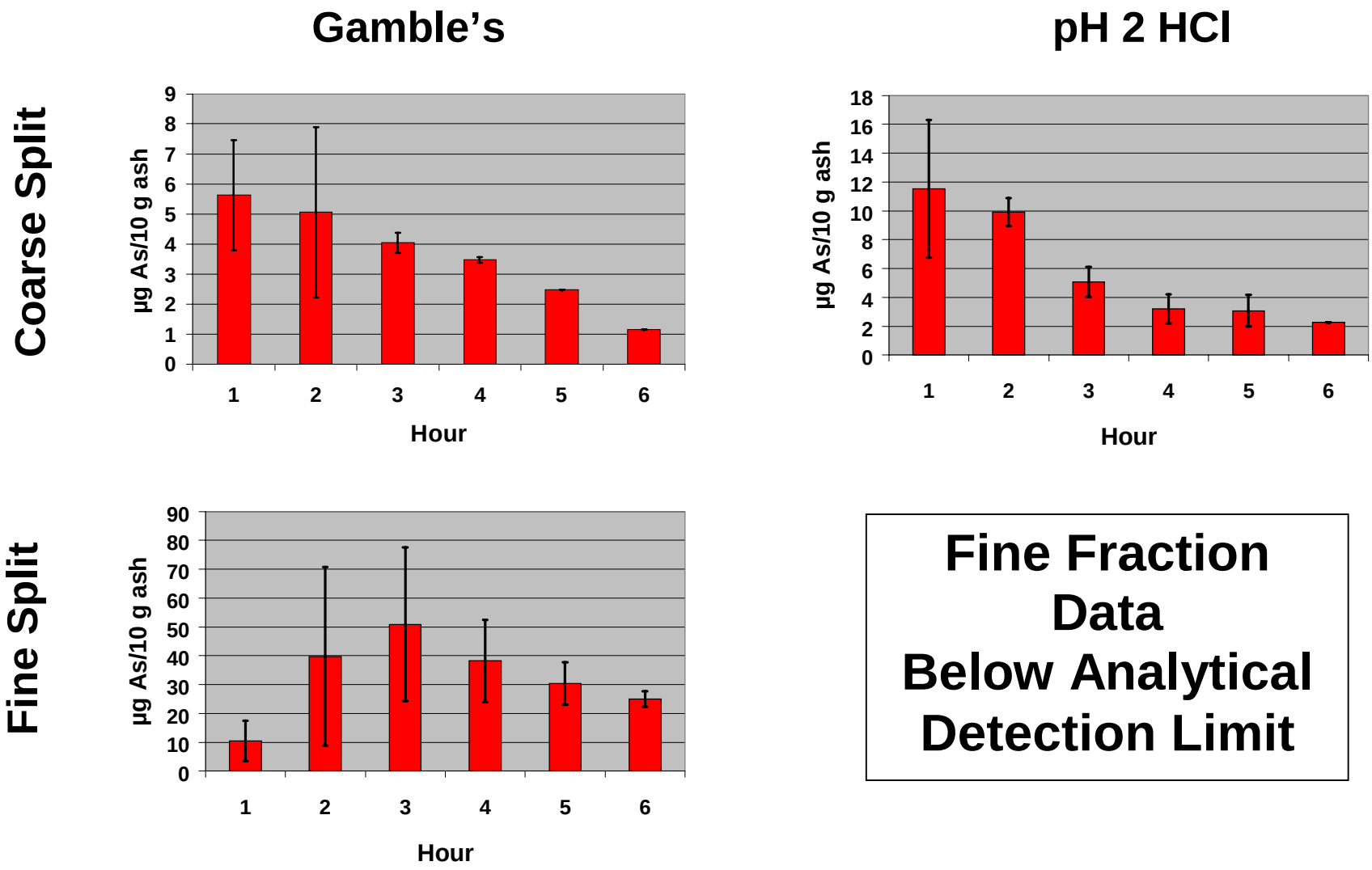

FIGURE 5. Hourly arsenic time release profiles determined from the analytical results are shown. The experimental results reported in Table 3 were normalized to determine hourly release rates (Table 4). Error bars indicate 1 σ errors when multiple data were available. These time release profiles were used to estimate the release of arsenic to the body from inhaled coal ash dust. The profile of the coarse fraction in pH 2 HCl was used for arsenic release to the stomach and the profile of the fine split in Gamble's solution was used to model arsenic release into the lung.

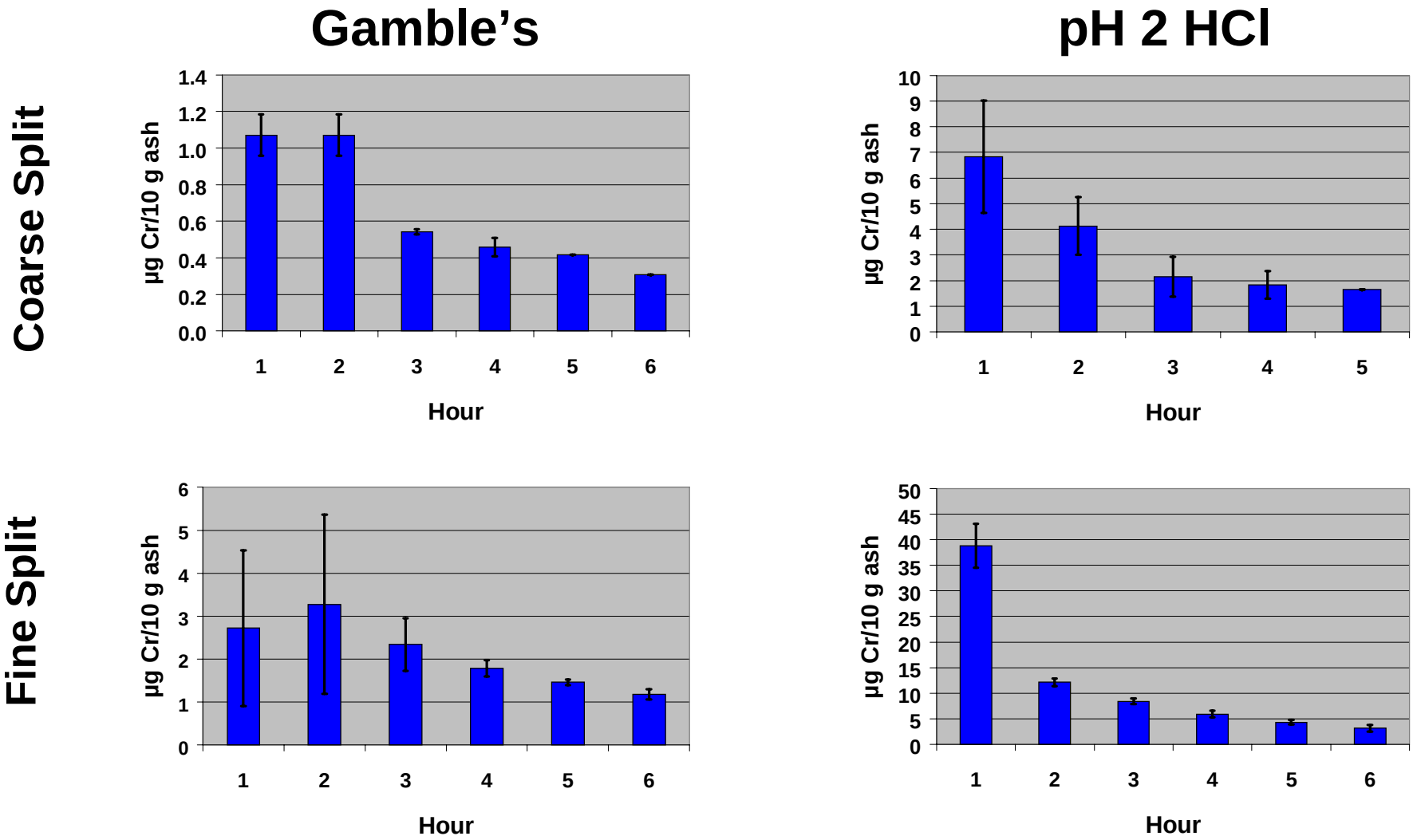

FIGURE 6. Hourly chromium time release profiles determined from the analytical results are shown. The experimental results reported in Table 3 were normalized to determine hourly release rates (Table 4). Error bars indicate 1 σ errors when multiple data were available. These time release profiles were used to estimate the release of chromium to the body from inhaled coal ash dust. The profile of the coarse fraction in pH 2 HCl was used for chromium release to the stomach and the profile of the fine split in Gamble's solution was used to model chromium release into the lung.

Model Input and Computation

The effects of a hypothetical dust exposure to our sample coal fly ash were evaluated. The dose model presented below assumes a 10 m^3 volume of respired air for an 8 hour work shift of moderate activity (ICRP, 1975). For the purpose the model, it was assumed that a worker was exposed to 10 mg/m^3 of the sample coal fly ash (100 mg/8 hour shift). The weight percentages of the fine and coarse splits were obtained from the size distribution characterization of each split. These data were used to determine the weight percent of inhaled ash deposited into the deep lung (fine split) and onto the upper respiratory system (coarse split). The size distribution data indicated that 62% of the ash was in the coarse split and 38% was in the fine split. A 70% deposition efficiency was assumed for the fine ash split. It was further assumed that 100% of the coarse inhaled split was deposited in the pulmonary system and subsequently translocated to the digestive system. A two hour linear offset was used between exposure and deposition of the coarse split and release to the digestive system as an estimate of the exposure delay due to transit time on the mucociliary escalator. This was to accommodate the time period for transfer of the coarse particulate matter to the gut. Some of the larger particles may reside in the respiratory system for longer periods of time (Snipes, et al., 1997). It was assumed that release of metals from the coarse split during this time period was insignificant.

Our model was constructed using a computer spreadsheet, and included arsenic and chromium contributions from occupational ash exposures and other environmental pathways. The occupational contribution of arsenic and chromium from our coal fly ash sample was made assuming occupational dust exposure for 8 hours per day, followed by a 16 hour hiatus from occupational exposure. Occupational exposures were further assumed to occur over five consecutive work days, with a two day break from exposure on weekends. The model accommodated hourly inputs of metal (in units of ng/hr) from coal ash into pulmonary and gastric compartments, defined by the results of our experiments (see Figures 5 and 6). It was assumed that the arsenic and chromium released from the ash into the lung and stomach was taken

up into the circulatory system for distribution and elimination from the body. For reference, environmental inputs from air, food, and water were integrated on an hourly basis and were considered to occur evenly over the 24 hour period, seven days per week. These environmental inputs were considered to be taken up into the circulatory system immediately upon administration. The model predicted the exposure impacts on the dynamic compartment of arsenic and chromium maintained from the competing effects of continuous dose administration and the concentration dependent clearance of these elements from the body. The amount of arsenic and chromium maintain in this dynamic compartment is much less than the amount of arsenic and chromium contained in the whole body. (ICRP, 1975, Lentner, 1981). A relational schematic of model components is shown in Figure 7.

Descriptive triphasic (three compartment) models incorporating mathematical reservoirs were used to calculate the clearance of arsenic and chromium from the body for our model. These clearance equations were of the general form

$$C_R = C_1 e^{-k_1 t} + C_2 e^{-k_2 t} + C_3 e^{-k_3 t}$$

where C_R is the amount of arsenic remaining after t hours. For calculation of hourly changes, t was equal to one hour. C_1, C_2, and C_3 are the concentrations of arsenic or chromium in each mathematical reservoir. The elimination rate constant for each reservoir is k_I, where k equals the natural log of 2 divided by the half life, in hours. Half lives of 8 hours, 24 hours and 8 days for each of the three compartments were used to quantify the removal of arsenic from the body (ACGIH, 1996; Foa et al., 1987; Mealey et al., 1959). These half life values were derived from the elimination of radiolabelled arsenite administered intravenously to subjects and measured the elimination of arsenic via the circulatory system. These half life values were chosen to complement our measured rate of arsenic release to the lung and stomach, building on our assumption of the uptake of arsenic and chromium into the circulatory system following release from the particles as measured by our experiments. It was further assumed that there was an even and parallel distribution of arsenic into these compartments (C_1=C_2=C_3=0.33). The clearance was applied

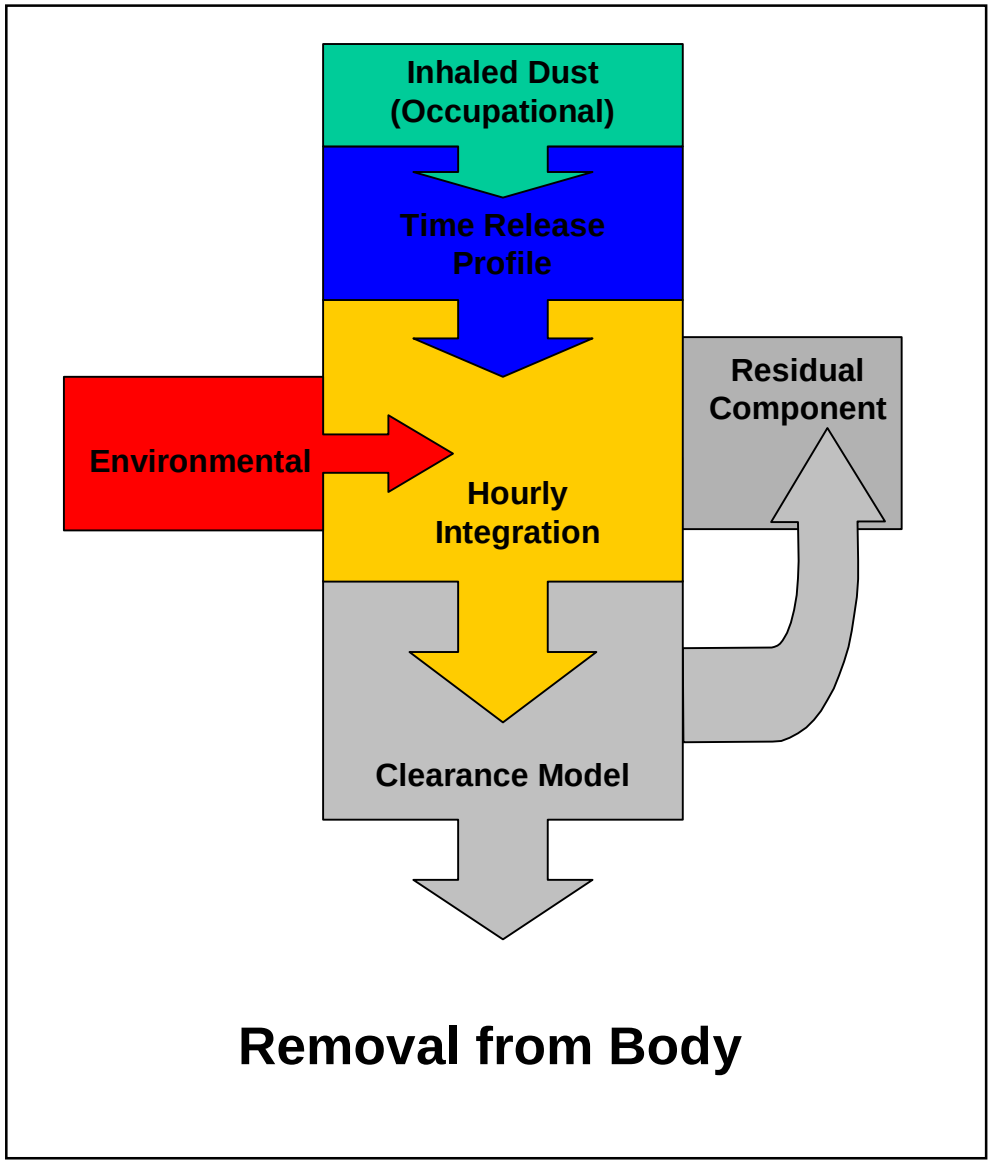

Figure 7. The schematic shows the relationship between components in the toxicokinetic model used in this report and shows the flow of information between components of the model. The time release profile data from our experiments (Figures 5 and 6, Table 4) were combined with estimates of coal fly ash dust exposures to provide the hourly occupational component of the arsenic and chromium dose. Environmental contributions from air, food, and water were determined from referenced sources (ATSDR, 1991a, b, WHO, 1983, and Bennett, 1986) and incorporated on an hourly basis. Triphasic clearance models were used to calculate the amount of arsenic and chromium removed from the body in an hour's time. The contributions from occupational and environmental sources were integrated on an hourly basis with the fraction of arsenic and chromium remaining from the clearance of the previous hour to calculated the arsenic in chromium "body burden". The model was used to calculate Figures 8-10.

to the calculated body burden from the previous hour increment. The remaining fraction was added to the most recent calculated hourly environmental and occupational inputs. Half-lives of 7 hours, 15 days, and 3 years were incorporated to quantify chromium elimination from the body (Aitio et al, 1988; ACGIH, 1993). As with arsenic, it was assumed that there was an even and parallel distribution of chromium into these compartments. The clearance rate was also applied to calculated body burden from the previous hour increment and added to the most recent calculated hourly input.

Model Results and Interpretation

Incremental and cumulative behavior of arsenic and chromium were studied using the model. Figure 8 shows predicted hourly incremental contributions from an initial 8 hour exposure to 10 mg/m^3 coal fly ash dust. Predicted release of metals to the body peaks 8 hours after first exposure then drops rapidly after the ash exposure stops. The solid lines in Figure 8 represent the accumulation of arsenic and chromium in the body. The failure of the cumulative curves to return to the pre-exposure baseline value indicates that both arsenic and chromium are predicted to accumulate through the work week, which is in agreement with the response observed in occupationally exposed groups (ACGIH, 1993; Buchet et al., 1981).

Two long term (four week) scenarios based on the model were also characterized. The first scenario shows occupational contributions of arsenic and chromium from 8 hour exposure, 5 consecutive days per week. These results are shown in Figure 9. The curves in Figure 9 show arsenic and chromium body burdens predicted for a four week period resulting from exposure to 10 mg/m^3 of the coal fly ash used in our experiments. The data show a rapid increase in body burden associated with initial exposure. A steady-state reservoir of arsenic and chromium is maintained by the competing effects of the occupational input and the concentration-dependent clearance model. An increase in arsenic and chromium body burdens results as exposure continues through the week. Our predicted output matched behavior observed in arsenic-exposed experimental and occupational cohorts (Buchet et al., 1981; ACGIH, 1993; ACGIH, 1996). The second scenario showed the results of addition of the environmental contributions of arsenic and chromium to the calculated occupational dose. The environmental contributions greatly

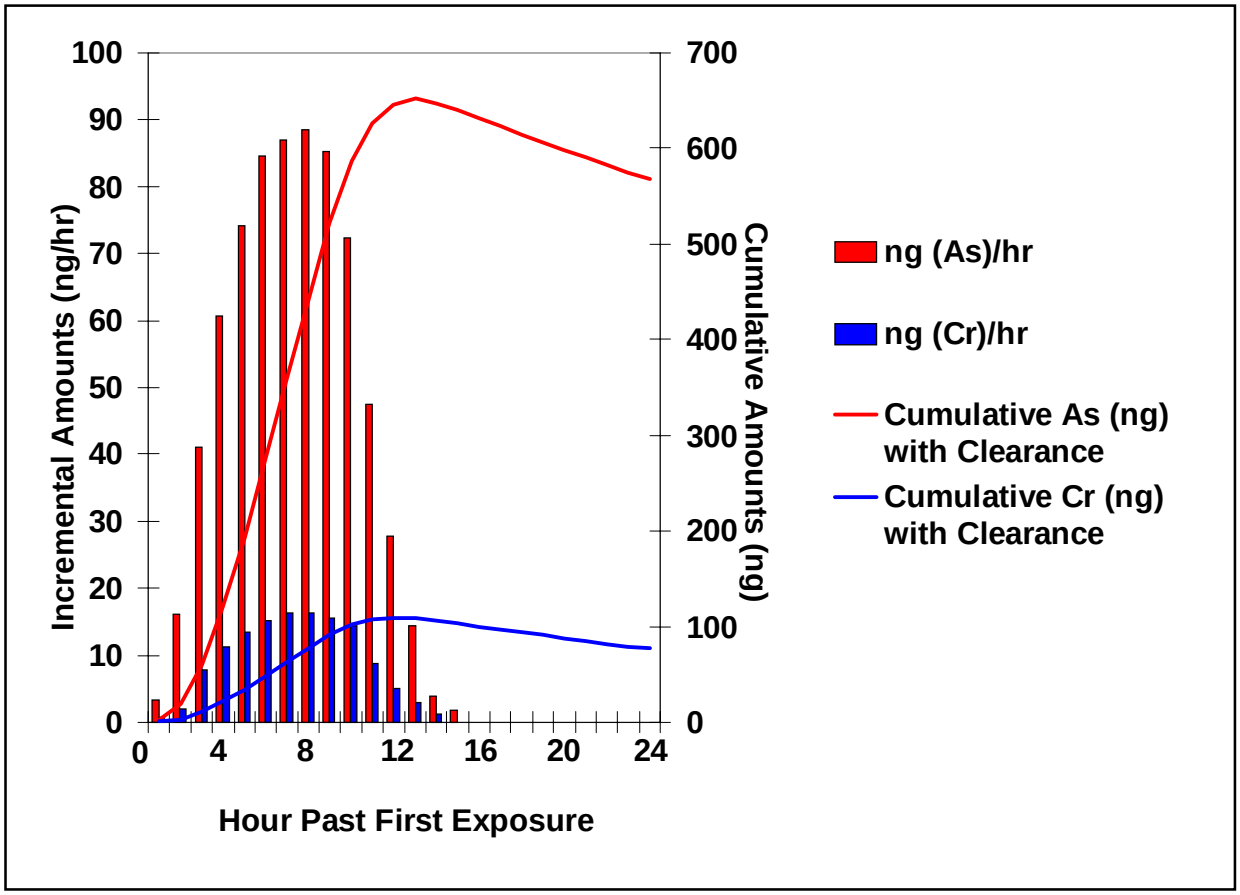

FIGURE 8. The figure shows the integrated hourly occupational contributions of arsenic and chromium from an 8 hour exposure to the coal fly ash used in the experiment at a dust concentration of 10 mg/m^3. Hourly contributions are shown by the bar chart data. The solid lines represent the calculated "body burden" resulting from application of the clearance model to the occupational input. Both arsenic and chromium would be expected to accumulate in the body through the work week, since the dose administered during the 8 hour work shift is not able to be cleared at the end of a 24 hour period.

outweigh the predicted contributions from inspired ash to the overall body burden. Figure 10 shows the predicted steady state body burden associated with environmental plus occupational exposure. The contribution of arsenic and chromium from predicted occupational exposure to coal fly ash is insignificant relative to the contribution from environmental sources. These results indicate that chromium and arsenic toxicity risk associated with exposures to the coal fly ash studied here would be of little concern.

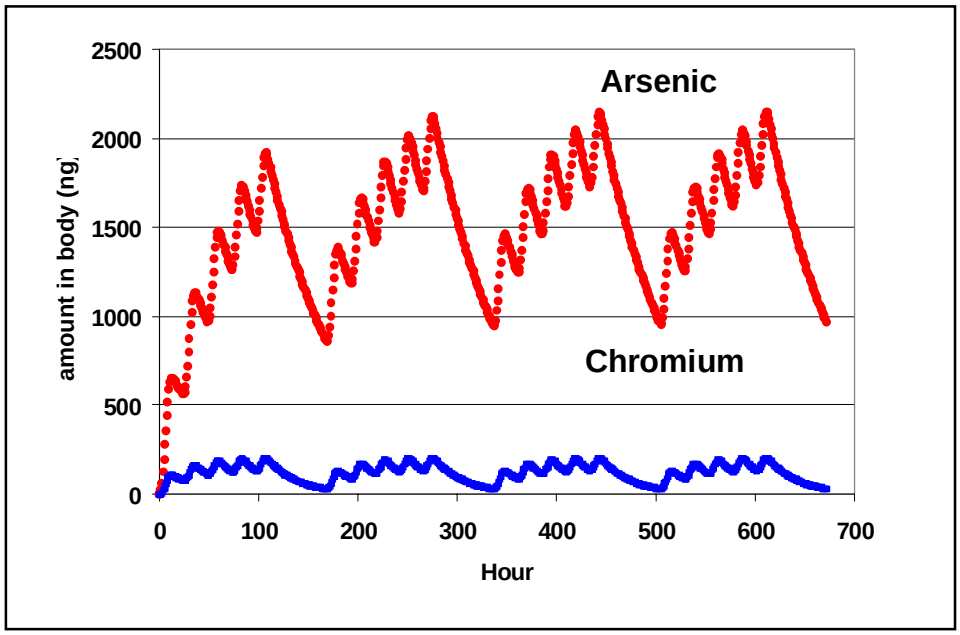

FIGURE 9. Predicted arsenic and chromium body burdens from a one month occupational exposure to 10 mg/m^3 (8 hours per day) of the coal fly ash sample used in our experiments assuming no other sources for these elements. A steady-state reservoir is maintained by the competing effects of the occupational input and the concentration dependent clearance model. Predicted contributions of arsenic from coal fly ash to the body exceed those of chromium.

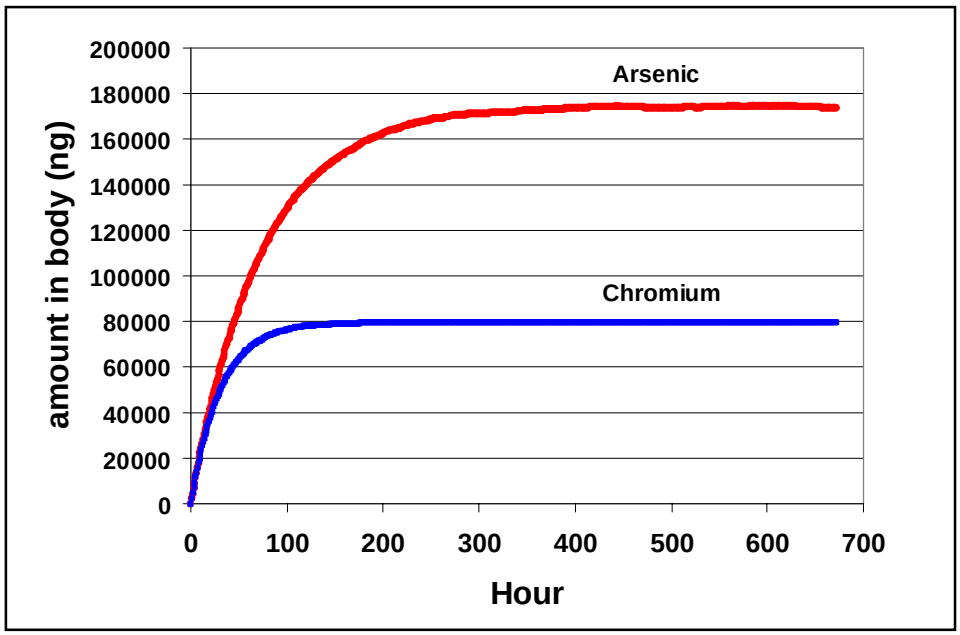

Figure 10. Predicted arsenic and chromium body burden over a one month period from both environmental pathways and occupational exposure to 10 mg/m^3 (8 hours per day) of the coal fly ash sample used in our experiments. Contributions of arsenic and chromium from environmental sources are considerably more significant than contributions received from occupational exposure to the test coal fly ash used on our experiments.

The predicted total amounts of arsenic and chromium defined by the model for occupational and environmental exposures represent a "dynamic compartment" defined by the difference between the amount of arsenic taken up from environmental and occupational sources and the amount of arsenic removed by the concentration dependent clearance from the body. These amounts of arsenic and chromium are considerably less than total amounts of arsenic and chromium stored in the body as a whole (ICRP,1975; Lentner, 1981). It is likely that under steady-state environmental and occupational exposure conditions, an equilibrium is achieved between the flux of elements through the body and physiologically-based storage reservoirs that may contain considerably greater absolute amounts of elements.

The time-release profiles from the geochemical experiments, combined with referenced clearance rates presented an estimate of the toxicokinetics of arsenic associated with exposure to coal fly ash. The comparison with biological monitoring data was performed to test the predicted clearance from the geochemical approach with actual exposure data documented in an occupationally exposed cohort. Results of the geochemical model were compared with biological monitoring data from a cohort exposed occupationally to fly ash from a high arsenic coal to evaluate the predictive capability of the geochemical characterization of the ash with industrial hygiene data. Urinary arsenic elimination was correlated with time weighted average arsenic breathing zone concentrations in a study of workers exposed to fly ash from arsenic rich coal (Yager et al, 1997). The comparison between the results of our geochemical investigation and toxicokinetic model and the results of the occupational exposure study was achieved through the following steps that served to recast our data in terms of the "x and y" variables used in the occupational exposure study.

1. The amount of arsenic removed from the body (based on our model) over a five day work week was determined by integrating the amount of arsenic removed hourly using our clearance equation.

2. The amount of arsenic eliminated through the urine over a five day work week was determined from the total amount of arsenic removed during the five day work week, assuming 60% of the arsenic eliminated from the body was removed via the urine (ACGIH, 1993, Buchet, 1981).
3. The amount of arsenic removed through the urine during the five day work week was normalized against referenced values for the weight of creatinine produced during a five day period to calculate the "creatinine normalized" arsenic elimination (a standard industrial hygiene approach).
4. The 8 hour time weighted average arsenic exposure that would result from an 8 hour exposure to the coal ash used in our study at a dust concentration of 10 mg/M^3 was calculated from the size characterization data and results of the arsenic analysis of the individual size splits.
5. The creatinine normalized arsenic elimination predicted from our model was compared with the creatinine normalized arsenic elimination predicted from the correlation established in the cohort occupationally exposed to high-arsenic coal fly ash, based on the arsenic 8 hour time weighted average concentration calculated from a 10 mg/M^3 exposure to our coal fly ash.

Data were presented that correlated urinary arsenic elimination with airborne arsenic time weighted average breating zone concentrations (Yager et al., 1997). Regression of 8 hour TWA breathing zone air samples against the creatinine normalized 5 day mean sum of arsenic metabolites (As_i, MMA, DMA) concentration yielded the following equation

$$As_{Urine} = 12.22 + 0.10\,As_{TWA}$$

where As_{urine} is the sum of creatinine normalized arsenic metabolites (μg As/g creatinine) and As_{TWA} is the 8 hour breathing zone concentration ($\mu g/m^3$) (Yager et al., 1997). The baseline urinary arsenic metabolite concentration predicted by this regression in the Slovak workers equals 12.22 μg As/gram creatinine. This would occur when urinary arsenic originated strictly from environmental sources, and the value of the occupational arsenic exposure (As_{TWA}) was zero.

The bioavailable fraction of arsenic predicted from our geochemical model was calculated as the average daily amount of arsenic removed from the body over the 5 day work week and was found to equal 0.38 μg As/day. Assuming that 60% of the arsenic was removed through the urine, 0.23 μg As/day would appear to be removed through the urine. Calculated urinary arsenic concentrations from our study were normalized against a range of creatinine elimination rates of 1.46-1.8 g/day, yielding estimated creatinine-normalized occupational arsenic elimination rates of 0.13-0.16 μg As/g creatinine.

Estimated arsenic exposures (as an 8 hour time-weighted average) were calculated from our coal fly ash bulk arsenic analysis (Table 1) and the weight fractions of fine and coarse ash. The 8 hour time-weighted average arsenic exposure associated with a 10 mg/M^3 coal ash dust exposure is 0.3 μg/M^3. The predicted urinary arsenic concentration from this occupational exposure (0.3 μg As /M^3) from the Yager et al. regression, neglecting baseline environmental contributions (y intercept value from the regression was set equal to zero), is 0.03 μg As/g creatinine.

The combination of the measurement arsenic release from the coal ash and the clearance model yields a reasonable first order approximation of the biological exposure when compared with the data from the occupationally exposed cohort (0.13-0.16 μg As/g creatinine versus 0.03 μg As/g creatinine). The estimates from our model are within a factor of 4-6 of the observed creatinine normalized urinary arsenic concentrations documented in occupationally exposed workers. The results of our study are considered in good agreement with the data from the occupationally exposed cohort, given the uncertainties in measuring exposure through biological samples, measuring air concentrations with industrial hygiene sampling and analysis techniques, and the experimental errors associated with our geochemical measurements. This favorable comparison supports the application of the geochemical techniques as estimators of biological exposure in this situation.

Although our approach endeavored to provide a reasonable estimate of potential arsenic exposures associated with the coal ash, future improvements in the technique could enhance the predictive capability of this method. The number of replicates performed on each series of experiment was considered sufficient to characterize the release behavior of arsenic and chromium from the ash considering the range of variability inherent in the measurement of exposure from biological samples. Application of a batch reactor technique might provide a more precise description of the shape of the release profile with time by permitting collection of samples at shorter time intervals, but would not likely change the measurement of the amount of arsenic or chromium released from the coal ash. A better test of the predictive capability would be to combine these geochemical experiments with an industrial hygiene evaluation of worker exposures under field conditions. This would eliminate the variability inherent in using one ash to characterize geochemical behavior then extrapolating the results to predict behavior from exposure to a second material. Ideally, both the geochemical and industrial hygiene exposure evaluations should be performed on the same agent.

CONCLUSIONS

The mixed flow reactor successfully determined the time release profiles of arsenic and chromium from the fine and coarse ash splits under conditions expected for human pulmonary and gastric environments. This permitted us to develop a detailed description of the timed release of arsenic and chromium to the body from respired ash fractions. The close agreement between the biological monitoring data of Yager et al. (1997) and our model demonstrates the effectiveness of applying geochemical techniques towards solving industrial hygiene exposure problems.

Our data indicate only minor amounts of arsenic and chromium were released from our sample of coal fly ash. The amounts of arsenic and chromium released from the ash under simulated physiological conditions were not significant enough to warrant separate consideration of chromium and arsenic

exposure. This particular coal fly ash should be considered no more than a nuisance dust for exposure control.

The geochemical approach permits evaluation of the behavior through time of a range of toxic agents that might be released from a complex substance. Estimating this behavior for *in situ* conditions allows the prediction of the potential dose resulting from exposure to the complex material. It is recommended that future studies should incorporate similar evaluation of the geochemical behavior of complex materials with biological monitoring of exposed cohorts.

ACKNOWLEDGMENTS

ICP support was provided through HP Environmental Laboratories, Inc. of Herndon, Virginia and the use of the transmission electron microscope was provided by Mantech Environmental Corporation, of Rockville, Maryland. The assistance of Dr. Hugh Granger (HP) and Mr. Mark Watson (Mantech) is greatly appreciated.

REFERENCES

ACAA (1998) "1996 Coal Combustion Product (CCP) Production and Use (Short Tons)" Hendl, K.B. "Internet Resources of Nursing Students." The American Coal Ash Association, Inc. <http://www.acaa-usa.org/whatsnew/ccpcharts.htm > (April 13, 1998).

ACGIH (1997) TLVs® and BEIs® Threshold Limit Values for Chemical Substances and Physical Agents Biological Exposure Indices, American Conference of Governmental Industrial Hygienists, Inc., 1997, Cincinnati, OH.

ACGIH (1996) Arsenic and soluble compounds, including Arsine. Supplement to the Documentation of the Threshold Limit Values and Biological Exposure Indices. 6th ed. vol 1-3. American Conference of Governmental Industrial Hygienists, Inc. Cincinnati, Ohio.

ACGIH (1993), Documentation of the Threshold Limit Values and Biological Exposure Indices. 6th ed. vol 1-3. American Conference of Governmental Industrial Hygienists, Inc. Cincinnati, Ohio.

Aitio, A., Jarvisalo, J., Kiilumen, M., et al. (1988) Chromium. in Biological monitoring of toxic metals, T.W. Clardson, L. Frieburg, G.F. Nordberg and P.R. Sager, eds. Plenum Press, New York.

Amdur, M.O., Doull, J., and Klassan, C.D., Eds. (1991) Casarett and Doull's toxicology: the basic science of poisons. 1033 p. Health Professions Division, McGraw Hill, Inc. New York, NY.

ATSDR (1991a) Toxicological Profile for Arsenic. United States Department of Health and Human Services.

ATSDR (1991b) Toxicological Profile for Chromium. United States Department of Health and Human Services.

Bennet, B.G. (1986) Exposure assessment for metals involved in carcinogenesis. IARC Sci Pub. 71 8:115-127.

Brunauer, S. Emmett, P. H., and Teller, E. (1938). Adsorption of gases in multimolecular layers. Journal of the American Chemical Society, 60, 309-324.

Buchet, J.P., Lauwerys, R., and Roels, H. (1981) Urinary excretion of inorganic arsenic and its metabolites after repeated ingestion of sodium metaarsenite by volunteers. International Archives of Environmental Health, 48:111-118.

Buchet, J.P., and Lauwerys, R. (1985). Study of inorganic arsenic methylation by rat liver in vitro: Relevance for the interpretation of observations in man. Archives of Toxicology, 57:125-129.

Buchet, J.P. and Lauwerys, (1988) Role of thiols in the *in vitro* methylation of inorganic arsenic by rat liver cytosol. Biochemical Pharmacol 37:3149-3153.

Davison, R.L., Natusch, D.F.S., Wallace, J.R., and Evans, C.A. (1974) Trace elements in fly ash – Dependence of concentration on particle size. Environmental Science and Technology, v. 8, no. 13, pp. 1107-1112.

EPRI (1994) Proceedings: Second International Conference on Managing Hazardous Air Pollutants, 1993. Winston Chow and Leonard Levin eds. Electric Power Research Institute, EPRI TR-104295,

Fisherova-Bergerova, V. (1990) Application of toxicokinetic models to establish biological exposure indicators. Annals of Occupational Hygiene, 34(6), pp. 639-651.

Foa, V., Columbi, A., Maroni, M., and Buratte, M., (1987) Arsenic. in Biological indicators for the assessment of human exposures to industrial chemicals. Commission of the European Communities, Luxembourg, 92p.

Gamble, James L., (1942) Chemical Anatomy, Physiology, and Pathology of Extracellular Fluid: A Lecture Syllabus. 6th Ed. Harvard University Press, Cambridge, Massachusetts, 164 p.

Grisafe, D.A., Angio, E.E., and Smith, S.M. (1988) Leaching characteristics of a high-calcium fly ash as a function of pH: a potential source of selenium toxicity. Applied Geochemistry, v. 3, pp. 601-608.

Hamel, S.G., Buckley, B, and Lioy, P.J. (1998) Bioaccessibility of metals in soils for different liquid to solid ratios in synthetic gastric fluids. Environmental Science and Technology, 32, pp. 358-362.

Hulett, L.D., Weinberger, A.J., Northcutt, K.J., and Ferguson, Marian (1980) Chemical species in fly ash from coal-burning plants. Science, 210, pp. 1356-1358.

ICRP (1975), International Council of Radiation Protection Report of the Task Group on Reference Man, No. 23., Pergamon Press, Elmsford, NY.

Jones, D.R. (1995) The leaching of major and trace elements from coal fly ash. in Environmenal aspects of trace elements in coal. Dalway J. Swaine and Fari Goodarzi eds. Kluwer Academic Publishers, Boston, MA. pp 221-262.

Lehnert, B. (1992) Defense mechanisms and particle-cell interactions. in Health Effects of Mineral Dusts. George Guthrie and Brooke Mossman, Eds. Mineralogical Society of America. 427-469.

Lentner, Cornelius, Ed. (1981) Geigy Scientific Tables, Volume 1. Medical Education Division, Ciba-Geigy Corporation, West Caldwell, NJ, 295 p.

Lerman S., Clarkson, T.W., and Gerson, R.J.(1983) Arsenic uptake and metabolism by liver cells is dependet on arseinc oxidation state. Chem Biol Interact 45:401-406.

Lund, L.G., and Aust, A.E. (1990) Iron mobilization from asbestos by chelators and ascorbic acid. Archives of Biochemistry and Biophysics, 278, 60-64.

Mealey, J., Brownell, G.L., and Sweet, W.H. (1959) Radioarsenic in plasma, urine, normal tissue, and intracranial neoplasms. Archives of Neruology and Psychiatry. v. 81 pp. 310-320.

Morrow, P.E., Gibb, F.R., and Gazioglu, K.M. (1967) A study of particulate clearance from the human lungs. American Review of Repiratory Disease. v. 96 no. 6, pp. 1209-1221.

Mossman, B.T. (1992) Cellular and molecular mechanisms of disease. in Health Effects of Mineral Dusts. George Guthrie and Brooke Mossman, Eds. Mineralogical Society of America. 513-521.

Pacyna, J.M (1986) Emission factors of atmospheric elements. in Toxic Metals in the Atmosphere, Jerome O. Nriagu and Cliff I. Davidson, eds. John Wiley and Sons, New York, pp, 1-32.

Pinto, S.S., Varner, M.O., Nelson, M.A., Labbe, A.L., and White, L.D. (1976) Arsenic trioxide absorption and excretion in industry. Journal of Occupational Medicine, v. 18, pp. 677-680.

Rimstidt, J.D., and Newcomb, W (1993) Measurement and analysis of rate data: The rate of reaction of ferric iron with pyrite. Geochimica and Cosmochimica Acta, 57, 1919-1934.

Scholze, H., and Conradt, R. (1987), An *in vitro* study of the chemical durability of siliceous fibres. Annals of Occupational Hygiene, v. 31, no 4B, pp. 683-692.

Smith, R.D., Campbell, J.A., and Nielson, Kirk K. (1979) Concentration dependence upon particle size of volatized elements in fly ash. Environmental Science and Technology, 13, pp 553-558.

Snipes, M.B., James, A.C., and Jarabek, A.M. (1997) The 1994 ICRP66 human respiratory tract dosimetry model as a tool for predicting lung burdens from exposures to environmental aerosols. Applied Occupaitonal and Environmental Hygiene. v. 12 no. 8. pp. 547-554.

Suloway, J.J., Roy, W.R., Skelly, T.M., Dickerson, D.R., Schuller R.M., and Griffin, R.A. (1983) Chemical and toxicological properties of coal fly ash. Environmental Geology Notes #105, Illinois Department of Energy and Natural Resources, 70 pp.

Szadkowski, D., Jorgensen, A., Essing, H.G., and Schaller, K.H. (1970) Creatinine elimination rate as a reference value for analysis of urine samples I: Effect of daily urine volume and circadian rhythm on creatinine excretion (in German). Zeitschrift fur Klinische Chemie und Klinische Biochemie, v. 8, no. 5, pp. 529-533.

USDOE (1997), Quarterly Coal Report: July-September, 1997. United States Department of Energy, Energy Imformation Administration, DOE/EIA-0121 (97/3Q) p. 52.

USEPA (1997) National Ambient Air Quality Standards for Particulate Matter, Final Rule (40 CFR Part 50) Federal Register: July 18, 1997 (Volume 62, Number 138)Page 38651-38701.

Vahter, M., Friberg, L., Rahnster, B., Nygren, A., and Nolinder, P., Airborne and urinary excretion of metabolites of inorganic arsenic among smelter workers. International Archives of Environmental Health. 57:79-91.

Vestergaard, P., and Leverette, R, (1958) Constancy of urinary creatinine elimination. Journal of Laboratory and Clinical Medicine v. 51, pp. 211-218.

Wadge, A., and Hutton, M. (1987), The Leachability and Chemical Speciation of Selected Trace Elements in Fly Ash from Coal Combustion and Refuse Incineration, Environmental Pollution, v. 48, pp 85-99.

Wallach, J.B. (1986) Interpretation of diagnostic tests: a synopsis of laboratory medicine, 4th ed. Little, Brown, & Company, Boston, MA, 825 p.

WHO (1983) 27th Report of the joint FAO/WHO expert committee on food additives. WHO Technical Report Series 696, v. 29, World Health Organization, Geneva.

Yager, J., Hicks, J., and Fabianova, E. (1997) Arirborne arsenic and urinary excretion of arsenic metabolites during boiler cleaning operations in a Slovak coal-fired power plant. Environmental Health Perspectives, v. 105, pp. 836-842.

CHAPTER 4: CONCLUSIONS

This dissertation presents two geochemistry methods that can be used to address industrial hygiene problems. A mixed flow reactor was used to characterize the behavior of minerals and mineral-like substances under body conditions in order to predict potential hazards associated with a respired dose of these substances. The mixed flow reactor was used to both measure the biodurability of a respirable mineral dust and to measure the bioavailability of elements from a respirable ash dust.

The first project used a mixed flow reactor to measure the biodurability of respired talc particles. It determined that the rate-limiting step in the dissolution of the mineral grain under lung conditions is the release of silica from the mineral's surface. The silica release rate from talc under simulated physiological conditions at 37°C was found to equal 1.4 ($\pm$ 1.1) x 10^{-11} mole Si / m^2 sec. This rate appears to be independent of solvent pH and composition, including the presence of organic chelators and protein at physiological concentrations. The estimated lifetimes of talc particles and other silicates in the lung were determined by applying a geometric shrinking sphere model that incorporates measured silica release rates. In all cases, the major factor controlling the estimate of particle lifetime was the release rate of silica from the mineral surface. Other factors such as particle geometry did not significantly affect biodurability estimates. The biodurability of silicates, controlled by the release of silica from the mineral surface, varies widely in the lung. One micron chrysotile particles dissolve in the lung within months, while similarly sized quartz particles remain over the life of the affected individual. Talc and olivine have intermediate silica release rates, and are predicted to dissolve over the period of several years.

The potential for a particle to cause disease is likely the product of several factors. Comparison of estimated lifetimes of talc particles with other magnesium silicates and silica phases suggests that biodurability alone does not define the potential of a mineral to cause disease. This indicates that other factors must be considered when evaluating the potential harmful effects associated with inhalation of

mineral dusts. Other properties related to the disease causing potential of a mineral dust likely include surface characteristics (such as the presence of sharp edges or the ability to generate free radicals) and the ability to induce a cellular or immune response upon deposition in the body. With these considerations in mind, use of biodurability estimates defined by these experiments can place constraints on disease models associated with inhalation exposure by defining upper bounds on the residence time of a particle in the lung.

The use of mixed flow reactor techniques to describe the bioavailability of elements from inhaled particles showed significant promise as a tool for industrial hygienists. Chapter 3 illustrates how the geochemical behavior of a complex, multi-element agent can be tied to the biological response of an occupationally exposed cohort. The mixed flow reactor data collected from samples of coal fly ash provided time release profiles of arsenic and chromium into physiological solvents that mimic the chemistry of the stomach and lungs. The mixed flow reactor technique readily measured effects of differences in both particle chemistry (based on the different measured time release profile of the two particle size fractions) and solvent chemistry on the release rates of arsenic and chromium from the fly ash. These release rates were integrated into a toxicokinetic model that approximates the biological response to various dust exposures. This study showed that the risks from arsenic and chromium exposure associated with inhalation of this particular coal fly ash were minimal, especially when compared with predicted daily doses received through environmental pathways.

The use of the mixed flow reactor was best suited for the determination of biodurability, although satisfactory results were obtained in its use for characterizing bioavailability. The biodurability measurements on talc were made after the reactor system had reached steady state after several hours of time. The data collected early in these biodurability measurements was for reference only, and not used in the biodurability measurement. This was in contrast to the characterization of arsenic and chromium bioavailability from coal fly ash, in which data were collected from the start of the experiment. The time

required to collect 30 mL of effluent limited the resolution of the time release profile curve in the bioavailability determinations. Use of a batch reactor, in which samples could be drawn at more frequent time intervals, would possibly enhance resolution of the shape of the time release profile. However, since all the effluent from the reactor was collected in the mixed flow reactor approach, determination of the total amount of arsenic and chromium release from the coal ash was not affected.

The experimental methods presented in this work provide a useful tool for the prediction of the biological response caused by exposure to complex respirable dusts. The geochemical techniques combined with the toxicokinetic model links exposure to complex agents with resulting biological effects. This approach has significant potential to provide valuable information about the potential hazards associated with exposure to a wide range of materials at a fraction of the cost and time associated with standard inhalation toxicology studies. A traditional inhalation toxicology study may take many months to years, hundreds of thousands of dollars, and involve the sacrifice of a large number of animals. The techniques described in this paper can be completed in a time frame of weeks to months, at a cost of several thousand dollars. The toxicokinetic model presented in Chapter 3 can be easily modified to account for the clearance for other materials such as lead and cadmium by incorporation of appropriate half-life estimates and could then be applied to study exposures to substances such as lead-based paint debris or welding fumes. Time release profiles of elements from other respirable dusts and fumes collected in the field can be defined using the mixed flow reactor technique, then compared with observed behavior in the exposed cohort. Actual side by side comparisons of the release rates of elements measured with the mixed flow reactor and the rates of biological clearance under field conditions would provide a valuable refinement of this application and would further efforts to eliminate overexposures to toxic metals before they occur.

VITA

Joseph B. Jurinski was born in Greenport, New York on September 5, 1964. He received a Bachelor of Science degree 1987 and a Master of Science degree in 1990 from Virginia Tech, then went to work as an industrial hygienist with NuChemCo, Inc. He began part-time work on his Ph.D. in 1993 seeking to combine his academic training in the geological sciences with the practice of industrial hygiene. During the time he worked on his doctoral research program, he was certified in the comprehensive practice of industrial hygiene by the American Board of Industrial Hygiene, and also certified to practice as a Virginia Certified Professional Geologist by the Commonwealth of Virginia Board for Geology. He returned to full time practice as an industrial hygienist with NuChemCo, Inc. after completing his degree in June, 1998.